UNIVERSIDADE FEDERAL DE SÃO CARLOS
CENTRO DE CIÊNCIAS EXATAS E DE TECNOLOGIA
DEPARTAMENTO DE QUÍMICA
PROGRAMA DE PÓS-GRADUAÇÃO EM QUÍMICA

# "EVALUATION OF THE BIOLOGICAL ACTIVITY OF THE DISINTEGRIN-LIKE AND CYSTEINE-RICH DOMAINS OF BOTHROPASIN, A METALLOPROTEINASE FROM BOTHROPS JARARACA"

**OLAMIDE TOSIN OLAOBA***

Dissertation presented as part of the requirements to obtain the title of MASTER IN CHEMISTRY, concentration area: CHEMISTRY.

**Advisor: Prof. Dr. Dulce Helena Ferreira de Souza**

***CAPES Scholar**

**São Carlos – SP**
**2021**

**UNIVERSIDADE FEDERAL DE SÃO CARLOS**

Centro de Ciências Exatas e de Tecnologia
Programa de Pós-Graduação em Química

## Folha de Aprovação

Defesa de Dissertação de Mestrado do candidato Olamide Tosin Olaoba, realizada em 17/05/2021.

### Comissão Julgadora:

Profa. Dra. Dulce Helena Ferreira de Souza (UFSCar)

Profa. Dra. Heloisa Sobreiro Selistre de Araujo (UFSCar)

Prof. Dr. João Renato Carvalho Muniz (IFSC/USP)

O presente trabalho foi realizado com apoio da Coordenação de Aperfeiçoamento de Pessoal de Nível Superior - Brasil (CAPES) - Código de Financiamento 001.

O Relatório de Defesa assinado pelos membros da Comissão Julgadora encontra-se arquivado junto ao Programa de Pós-Graduação em Química.

# Dedication

This work is dedicated to the loving memory of my mother, Late Mrs. Olayinka Funmilola Olaoba. She will forever live in the heart of men.

## Acknowledgement

First, Glory be to God Almighty for the grace bestowed and the success of this work.

The 35th U.S president John F. Kennedy said “Effort and courage are not enough without purpose and direction”; the purpose and direction of this work were chiefly provided by my revered advisor, Professor (Dr.) Dulce Helena Ferreira de Souza. Prof. Dulce did not only supervised me, but she was also actively involved in mentoring my academic growth. For all of these, I am indebted to her than I could pay; I sincerely appreciate the opportunity.

Further, I recognize the collaborative impact of Professor (Dr.) Heloisa Sobreiro Selistre-de- Araujo of the Department of Physiological Sciences, UFSCar for providing access into her laboratory for the cell adhesion and inhibition assays. In like manner, I acknowledge the support of Dr. Kelli C. Micocci of UNESP, Rio Claro for providing guidance during the cell adhesion assays.

I am grateful to my thesis committee (Professor Heloisa Sobreiro Selistre-de- Araujo, Professor Joao Renato Muniz, and Professor Felipe Christoff Wouters) first for accepting to be members, second for their constructive critiques, and their support through the entire period.

One major factor that influenced the success of this work is a conducive work environment. The atmosphere provided by my colleagues in the laboratory was a type that support rapid growth. I am particularly indebted to Katia Celina Santos Correa for our rapport and her immense support during the development of this work. I am also grateful to several

others including Bruna Soares, Jessica Patty, and Amanda Sanchez for the memories we shared.

This work was supported by funding bodies to whom I am grateful. I acknowledge the Coordenação de Aperfeiçoamento de Pessoal de Nível Superior - Brasil (CAPES) - Finance Code 001 for financing this work in part. I am also thankful to CNPq and FAPESP for providing grants to support works in the laboratory.

Moreover, I sincerely gratify all professors in the “Departamento de Quimica” who cultivated values and academic cultures in me during the classes I took. My appreciation is also extended to UFSCar community at large.

The 17th – century English Philosopher Thomas Hobbes said “Leisure is the mother of philosophy”. My leisure was fulfilling with the companion of my West African Brothers – Dr. Bolaji Charles; Elijah Anertey; Amos Akinyemi; Kehinde Ayinde; John Teiboh; Zaccheaus Alabi. I am also grateful for the “*esprit de corps”* of my scientific brothers across the world – Oluwatosin Saibu; Adekunle Adebayo; Michael Akintubosun; Lateef Michael; Oluwatobi Ajayi.

Finally, I recognize the continuous impact of my father, Mr. Samuel S. Olaoba and my Siblings (Morenike Olaoba, Grace Olaoba, and Emmanuel Olaoba) for their unending love, prayers, support, and encouragement.

## List of Abbreviations

| | |
|---|---|
| **ADMIDAS:** | Adjacent MIDAS |
| **DAPI:** | $4^1$, 6-diamino-2-phenylindole |
| **ECM:** | Extracellular matrix |
| **GAGs:** | Glycosaminoglycans |
| **GST:** | Glutathione S transferase |
| **HUVECs:** | Human umbilical vein endothelial cells |
| **IMAC:** | Integrin mediated adhesion complex |
| **IPTG:** | Isopropyl – β – D - thiogalactopyranoside |
| **LB:** | Luria-Bertani |
| **MIDAS:** | Metal-ion depended adhesion site |
| **OD:** | Optical density |
| **PBS:** | Phosphate buffered saline |
| **SDS-PAGE:** | Sodium dodecyl sulfate polyacrylamide gel electrophoresis |
| **SVMPs:** | Snake venom metalloproteinases |
| **SyMBS:** | Synergistic metal-ion binding site |
| **VLA-2:** | Very late activation antigen-2 |

# List of Figures

# Abstract

EVALUATION OF THE BIOLOGICAL ACTIVITY OF THE DISINTEGRIN-LIKE AND CYSTEINE-RICH DOMAINS OF BOTHROPASIN, A VENOM METALLOPROTEINASE FROM BOTHROPS JARARACA

Bothropasin is a 48kDa hemorrhagic class III Snake Venom Metalloproteinase (SVMP). As a multi-domain protein, it contains catalytic metalloproteinase (M), disintegrin-like (D), and cysteine rich domains (C). Integrins belong to the superfamily of transmembrane cell adhesion receptor that interact and bind to soluble ligands, cell-surface ligands, and extracellular matrix ligands such as collagen. The integrin-binding motif of bothropasin unlike the P-II members (that contain RGD-motif) is an ECD tripeptide. It was previously reported that cysteine (C) and aspartate (D) of the ECD were responsible for disulfide formation and calcium interaction respectively, while the glutamate (E) was found exposed to solvent and free to make interaction. Thus, we propose that (E) may also be responsible for integrin binding. Furthermore, in the current project, we intend to further ascertain the role of glutamate in integrin binding via the ability of this protein to inhibit adhesion of HUVECs (cell lines that can also express α2β1 integrin) to collagen1-coated wells. Previously in our group two clones were built to express the bothropasin DC domains (BDC) containing ECD motif (BDC-ECD protein) and the mutant ACD (BDC-ACD protein). The clones were transformed in *E. coli* (BL21(DE3) and DH5α) and the expression was induced by IPTG. The soluble fractions of the proteins were purified with affinity chromatography, analyzed with 15 % SDS-PAGE and western blotting; and we investigated the effect of glutamate mutation on the ability of these proteins (in fusion with GST) to inhibit cell adhesion. The result

showed that the proteins did not inhibit adhesion of HUVECs to collagen 1. Although the result indicate that pretreatment of HUVEC cells with GST GST only did not affect protein activities, there is a possibility that GST in fusion with this protein could interfere with protein native folding and culminate in protein inactivities. The current data thus suggest the use of proteins free from GST for further studies.

# Resumo

AVALIAÇÃO DA ATIVIDADE BIOLÓGICA DOS DOMÍNIOS TIPO-DESINTEGRINA E RICO EM CISTEÍNA DA BOTROPASINA, UMA METALOPROTEINASE DE BOTHROPS JARARACA

A botropasina é uma proteína hemorrágica de 48 kDa da classe PIII das Metaloproteinase de veneno de serpentes (SVMP). Como uma proteína de múltiplos domínios, ela contém o domínio catalítico, domínios do tipo desintegrina e rico em cisteína. As integrinas pertencem à superfamília de receptores de adesão celular transmembrana que interagem e se ligam a ligantes solúveis, ligantes de superfície celular e ligantes de matriz extracelular, como o colágeno. O motivo de ligação à integrina da botropasina, ao contrário dos membros P-II (que contêm o motivo RGD), é um tripeptídeo ECD. Foi relatado anteriormente que a cisteína (C) e o aspartato (D) do ECD foram responsáveis pela formação de dissulfeto e interação de cálcio, respectivamente, enquanto o glutamato (E) foi encontrado exposto ao solvente e livre para fazer interação. No presente trabalho pretendemos averiguar a função do glutamato (E) na ligação (e na inibição) da proteína à integrina α2β1, expressa por células HUVECs. Previamente em nosso grupo dois clones foram construídos para expressar os domínios DC da botropasina (BDC) contendo o motivo ECD (proteína BDC-ECD) e o mutante ACD (proteína BDC-ACD, onde o E foi mutado por alanina). Os clones foram transfomados em *E. coli* (BL21(DE3) e DH5α) e a expressão das proteínas foi induzida por IPTG. As frações solúveis das proteínas foram purificadas por cromatografia de afinidade, analisadas com SDS-PAGE 15% e Western blotting e investigamos o efeito da mutação do glutamato na capacidade dessas proteínas (em fusão com a GST) de inibir a adesão celular. O resultado mostrou que as proteínas não inibiram a adesão

de HUVECs ao colágeno 1. Embora o resultado indique que o pré-tratamento de células HUVEC com GST GST apenas não afetou as atividades da proteína, existe a possibilidade de que GST em fusão com esta proteína poderia interferir com o dobramento nativo da proteína e culminar em inatividades de proteínas. Os dados atuais sugerem, portanto, o uso de proteínas isentas de GST para estudos posteriores.

# Table of Contents

# 1.0 Introduction

## 1.1 Snake venom metalloproteinase

Snake venom metalloproteinases (SVMPs) are complex mixture of dissimilar proteins containing many domains (Fox and Serrano, 2009). They are species-specific enzymes possessing various biological activities which are highly dependent on zinc. The presence of zinc-proteinase in SVMPs impart a typical symptom development during envenomation including hemorrhage, hypovolemia, necrosis, inflammation, edema, and hypotension (Fox and Serrano, 2005). Chiefly, *Viperidae* family and *Crotaline* subfamily houses significant amount of SVMPs as compared to other families. However, their presence in venoms are critical to the ability of these snakes to adapt to their environment (Moura-da-Silva et al., 2016).

### 1.1.1 Classification of SVMPs and structural peculiarities

Over the years, the classification of SVMP has been controversial and thus, there have been continuous attempt to review and update the classification. For instance, the penultimate 4 group classification considered precursor mRNA sequences and or protein size purified from the venom (Bjarnason and Fox, 1994; Hite et al., 1994). In 2008, SVMP was classified into 3 groups namely P-I, P-II, and P-III (Fox and Serrano, 2008). The 2008 classification is the most recent classification of SVMPs. Although new features are found in newly isolated SVMPs, there exist some sub-classes that can house these features. In the future, the continuous discovery of more diversified SVMPs may create pressure on the current classification; therefore, the current classification is vulnerable to re-classification.

The smallest and the simplest of all the classes is the P-I class. Their molecular mass ranges from 20 to 30 kDa. Matured members of this class

only possess the metalloproteinase (M) domain. Interestingly, the biological activities of this class depends on the structural features of their M domain. One of the unique structural characteristics of the M domain is the presence of a unique zinc-binding sequence (HEXXHXXGXXH) and a 'Methionine-turn' motif. All these features confer important physiological role on P-I including their ability to degrade basement membrane components as well as hemorrhagic phenotype – *reviewed from Olaoba et al. (Olaoba et al., 2020).*

A moderately advanced class of SVMP called the P-II has an additional domain apart from the metalloproteinase domain that is observed in the P-I class. In fact, cDNA sequence analysis revealed that the full length of P-II SVMP contain a signal sequence, a prodomain, a metalloproteinase, and a disintegrin domain. In the matured form, members of the P-II only retain the metalloproteinase and the disintegrin domains (Camacho et al., 2014; Takeda et al., 2012). Due to the presence of an additional domain, the molecular mass of P-II proteins is higher than the P-I class. For those that have been described, their molecular mass fall within the range of 30 to 60kDa (Casewell et al., 2011). The complexity of this class might have arisen as a result of their predisposition to inter-domain cleavage (majorly the cleavage of disintegrin from the metalloproteinase domain). However, some members like abolamin and agkistin possess a unique reinforcement of two cysteinyl residues that protect them from proteolytic attack (Jangprasert and Rojnuckarin, 2014; Wang et al., 2003). Taken together, 5 subclasses of SVMP were specified in the most recent classification (Figure 1.1) and they include P-IIa, P-IIb, P-IIc, P-IId, and P-IIe (Fox and Serrano, 2008). Descriptively, the P-IIa represent a cleaved fragment of metalloproteinase domain that is entirely separated from another domain fragment – disintegrin. In the P-IIb, the domains are intact so that they are not further

processed. The P-IIb is a canonical form of P-II SVMPs; a matured P-IIb protein contains a metalloproteinase and a disintegrin domain. Furthermore, another subclass called the P-IIc arise as a result of the dimerization between two canonical P-II and are stabilized by Disulfide Bridge between their metalloproteinase domains. The possibilities of dimer formation involving disintegrins have been shown. The P-IId members are homodimeric disintegrins stabilized by Disulfide Bridge. Finally, a P-IIe class that involve two dissimilar disintegrins can form heterodimers (Olaoba et al., 2020). Like the P-I class, the domain composition of the P-II proteins is an important determinant of their biological activities. For instance, one important effect that can be attributed to the presence of a disintegrin domain is their ability to interact with integrins. Disintegrins of P-II contain distinct characteristics that enable them to bind integrins. Studies have identified the presence of conserved integrin-binding motif (RGD-motif) that reside in a flexible loop of 13 aminoacyl chain. Such interaction is capable of inhibiting platelet aggregation or cell adhesion (Danilucci et al., 2019; Masuda et al., 2000). Nevertheless, KGD, VGD, WGD, MLD, RTS, and KTS are the variants of the RGD- motif which as a result of these variation can add to their degree of diversity and impact their biological activities (Calvete et al., 2005; Cesar et al., 2019).

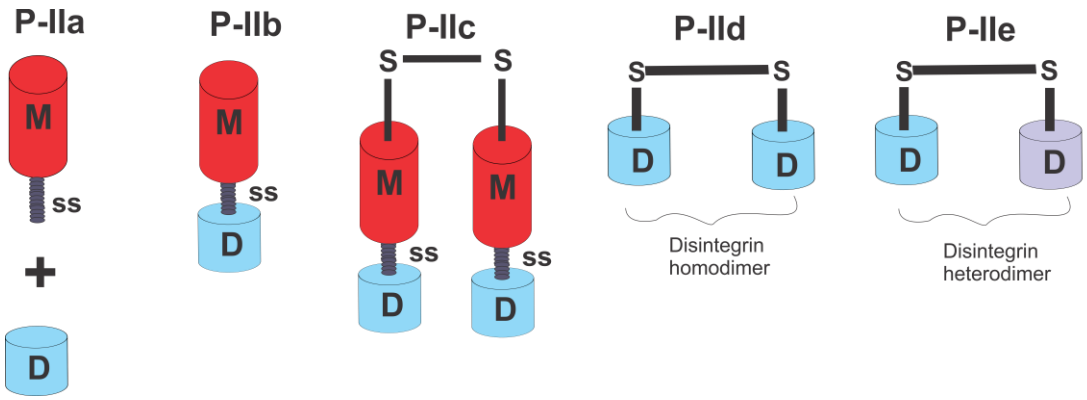


**Figure 1.1:** Representation of the sub-classification of P-II SVMPs (Olaoba et al., 2020).

The most complex and diversified class is the P-III proteins. They possess higher molecular mass that ranges from 60 to 100 kDa (Markland and Swenson, 2013). Canonical P-III proteins contain metalloproteinase, disintegrin-like, and cysteine-rich domains in their matured form. Beyond the canonical structure, there are other modifications that give rise to a sub-classification (Figure 1.2). In an extensive review, Olaoba and colleagues summarized the sub-classification of the P-III SVMPs. They include P-IIIa, P-IIIb, P-IIIc, P-IIId, and P-IIIe (Olaoba et al., 2020). The P-IIIa is canonical. In the P-IIIb subclass, there is a processed fragment of metalloproteinase domain entirely separated from another fragment of continuous disntegrin-like and cysteine-rich domains. On the other hand, dimerization of canonical P-III structures is a feature of the P-IIIc subclass and are stabilized by Disulfide Linkages. The constituent monomers may be homologous or heterologous and thus forming homo- and heterodimers. In addition to the canonical structure, the C-terminus of the cysteine-rich domain can undergo complexation with C-type lectin-like proteins, a characteristics of the P-IIId subclass. Lastly, in the P-IIIe class, the metalloproteinase domain is lost, so

that only the disintegrin-like and cysteine-rich domains are present (Olaoba et al., 2020). Importantly, the biological activities of this class are determined by the structural features of their domains. Most significantly, the disintegrin-like domain of the P-III class is so called because of the presence of a non-canonical integrin-binding motif. Although this motif (D/ECD) is non-canonical, it is conserved in the members of the P-III class.

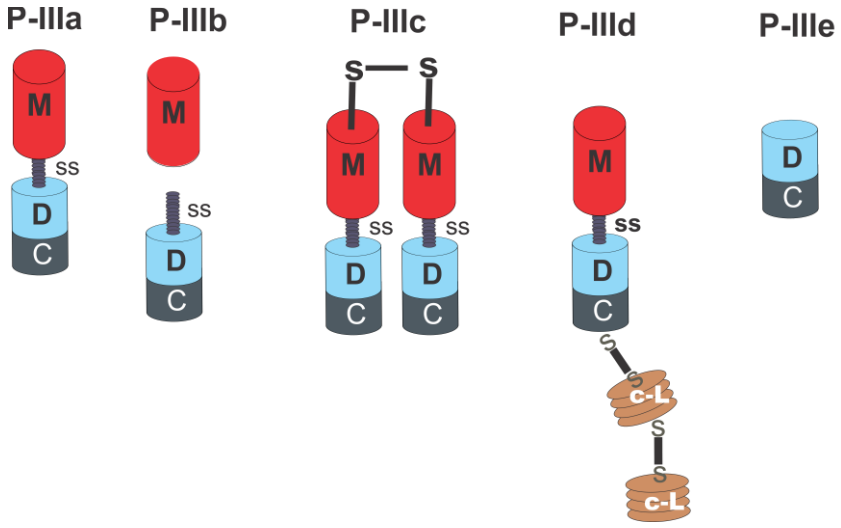


**Figure 1.2:** Representation of the sub-classification of P-III SVMPs (Olaoba et al., 2020).

## 1.1.2 Biological activities of SVMPs

The metalloproteinase domain is the most catalytically active domain of SVMPs. Other domains can elicit an independent role or promote the metalloproteinase activities of SVMPs. However, the metalloproteinase activities of P-I proteins differ from those of P-II and P-III proteins in that the hemorrhagic activities of P-II and P-III metalloproteinases are more pronounced than those of P-I proteins (Herrera et al., 2015). This hemorrhagic activities include the ability of these proteins to hydrolyze

basement membrane proteins – such as laminin and collagen – leading to bleeding (de Souza et al., 2016). On the other hand, the non-hemorrhagic metalloproteinases have been reported, most of whose activities are associated with fibrino(geno)lytic and induction of apoptosis (Baldo et al., 2008).

Furthermore, disintegrin and disintegrin-like domains are important features of the P-II and P-III proteins respectively. The biological role of these domains is marked by the presence of conserved motif in their sequence. Although the motif of P-II disintegrin differs from the P-III disintegrin-like, these motifs enable interactions with various integrins (Chang et al., 2017). However, such interaction may also have biological consequence including the inhibition of platelet aggregation (Ramos et al., 2008), inhibition of cell adhesion (Danilucci et al., 2019), inhibition of proliferation (Chalier et al., 2020), and induction of autophagy (Lino et al., 2019). Finally, the cysteine-rich domain that is peculiar to the P-III SVMPs can also impact their biological activities. Studies have shown that the functional association of the cysteine-rich domain with the disintegrin-like domain may play role in acute inflammatory response. In a particular report, such association caused leukocyte rolling and release of pro-inflammatory cytokines (Clissa et al., 2006).

## 1.2 Bothropasin: A class three SVMP

Bothropasin is a 48 kDa hemorrhagic P-III SVMP that is responsible for most snake bites in the Southeastern Brazil (Molina Molina et al., 2018; Muniz et al., 2008). Ammonium sulfate precipitation, DEAE-cellulose and DEAE-shephadex A-50 chromatographies; and shephadex G-100 column filtration were employed in the first isolation of bothropasin in 1982. The protein was isolated from the venom of *Bothrops jararca* (Mandelbaum et

al., 1982). Around this period, not many scientists were prepared to characterize bothropasin. Three years after its first isolation, the same group of scientists found out that the protein could cause hemorrhage, myonecrosis, and arterial necrosis following an intramuscular injection in mice (Queiroz et al., 1985).

For more than two decades, it appeared that one or more of the scientists who were involved in the initial isolation of bothropasin were also actively involved in the characterization. It is therefore no surprise that they also determined the full-length cDNA encoding the bothropasin precursor and could be cloned by immunoscreening. However, the bacterial, yeast, and mammalian cell expression system did not yield significant result. But the bacterial cell expression was used to study the individual domains of bothropasin; although as of this time, the metalloproteinase domain could not be expressed with the system (Assakura et al., 2003). It is also clear at this time that bothropasin belongs to the P-III class of SVMP. As the field of toxinology advances, scientists saw the need to avail alternative source of venom proteins other than obtaining them from the wild. Carneiro and colleagues maintained and characterized the secretory cell of *Bothrops jararaca* venom gland culture for 21 days. In those times, isolated cells were assembled into acini as they grow in size. By employing immunoelectron microscopy technique, bothropasin was shown to be localized in the secretory vesicle (Carneiro et al., 2006).

For the first time in 2008, the three dimensional structure of bothropasin was determined in complex with POL647 inhibitor (Figure 1.3).

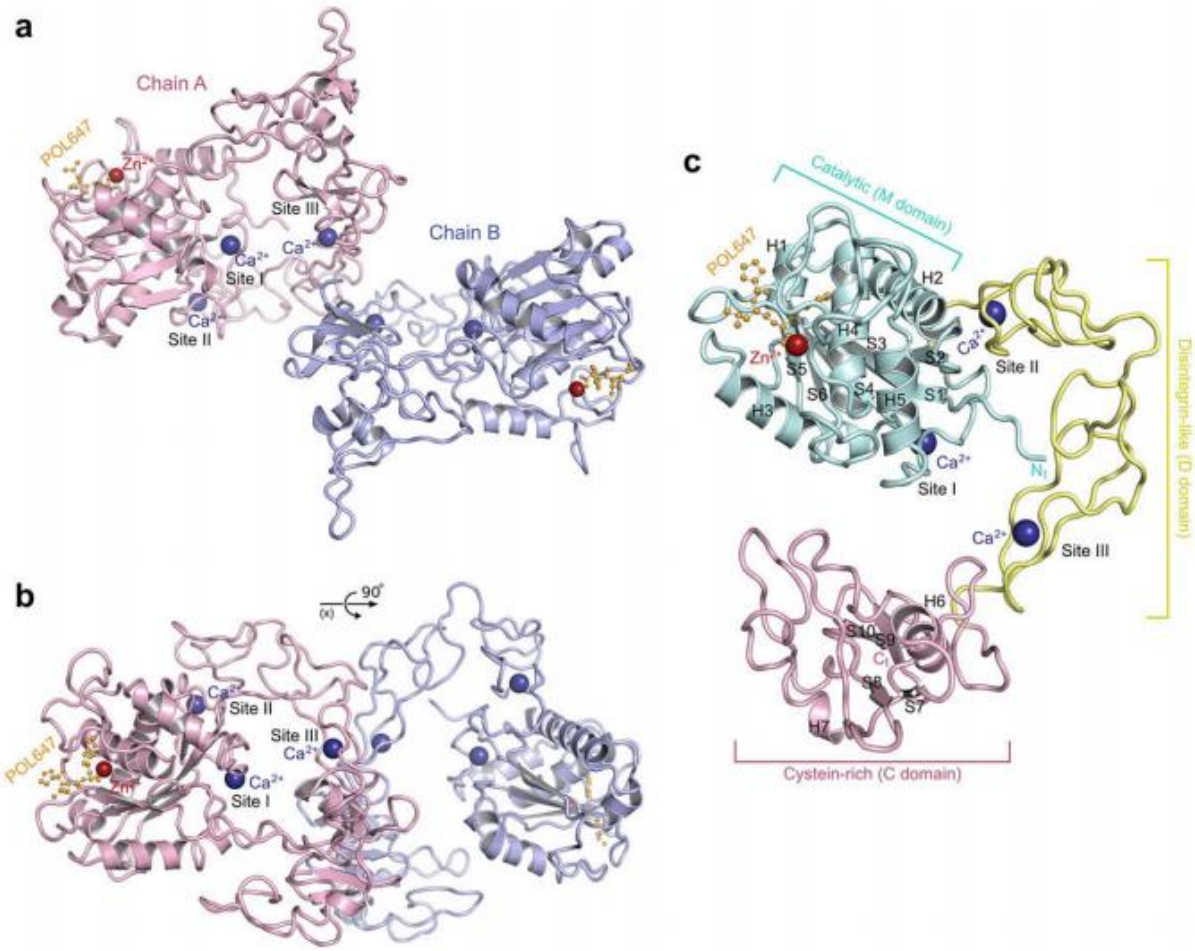


**Figure 1.3:** The overall structure of bothropasin in complex with POL647 inhibitor (Muniz et al., 2008).

The catalytic domain of bothropasin was shown to contain scaffold of two subdomains including zinc and calcium binding site (Muniz et al., 2008). The disintegrin domain of bothropasin contains loops that are stabilized by 7 disulfide bonds and two calcium ions. Additionally, a unique region that corresponds to the P-II RGD-motif was also identified in this structure. However, the region does not contain RGD tripeptide, but instead an ECD tripeptide that is embedded in a loop and stabilized by interdomain disulfide bond between $Cys^{278}$ of the disintegrin-like domain and $Cys^{310}$ of the

cysteine-rich domain. Despite the realization that the C (cysteine) and the D (aspartate) of the ECD were responsible for disulfide formation and calcium interaction respectively, the E (Glu276) was found exposed to solvent and free to make interaction. Finally, the hyper-variable region of the cysteine-rich domain also contain a well-conserved sequence in bothropasin as it were in some other P-III SVMPs (Muniz et al., 2008).

It is important to emphasize that bothropasin is a highly hemorrhagic protein, no wonder it is responsible for the systemic effect associated with bothropic envenomation. Such effect includes inflammation, necrosis, and blood coagulation deficiency (Molina Molina et al., 2018). To add to this hemorrhagic profile, research has underlined the ability of bothropasin to interact and degrade fibrinogen, fibronectin, laminin, collagens I and VI (Oliveira et al., 2010). In a more recent report, a B-cell epitope was identified in the catalytic domain of bothropasin (Molina Molina et al., 2018).

## 1.3 Integrins

Throughout the life span of an organism, there is a complex inter-cellular and intracellular events that are essential to the growth and development of that organism. Such cellular activities are biological processes that are marked by cell-matrix and cell-cell interactions. However, this interaction of cell with extracellular matrix components or a cell with another is mediated mostly by transmembrane integral receptor protein (Labat-Robert, 1992) that support cell anchorage and organismal architecture. These receptors are the integrins that are used by lower and higher eukaryotes to carry out this cellular assignment. Integrins belong to the superfamily of transmembrane cell adhesion receptor that interact and bind to soluble ligands, cell-surface ligands, and extracellular matrix ligands (Takada et al., 2007). The role of these receptors are also critical to sensing

and adherence to extracellular environment as they couple the extracellular environment to intracellular signals (Kadry and Calderwood, 2020).

Structurally, integrins contain two subunits – $\alpha$ and $\beta$ – which interact to form heterodimers. In human cells, 18α and 8β subunits are expressed and they can assort independently to form 24 different heterodimers (Figure 1.4). Each of the subunit is a type-I transmembrane protein that contain an extended extracellular multi-domain portion, a transmembrane region, and a short cytoplasmic tail (Hynes, 2002). The exact subunit combinations has been shown to impart ligand specificity and function (Humphries et al., 2006).

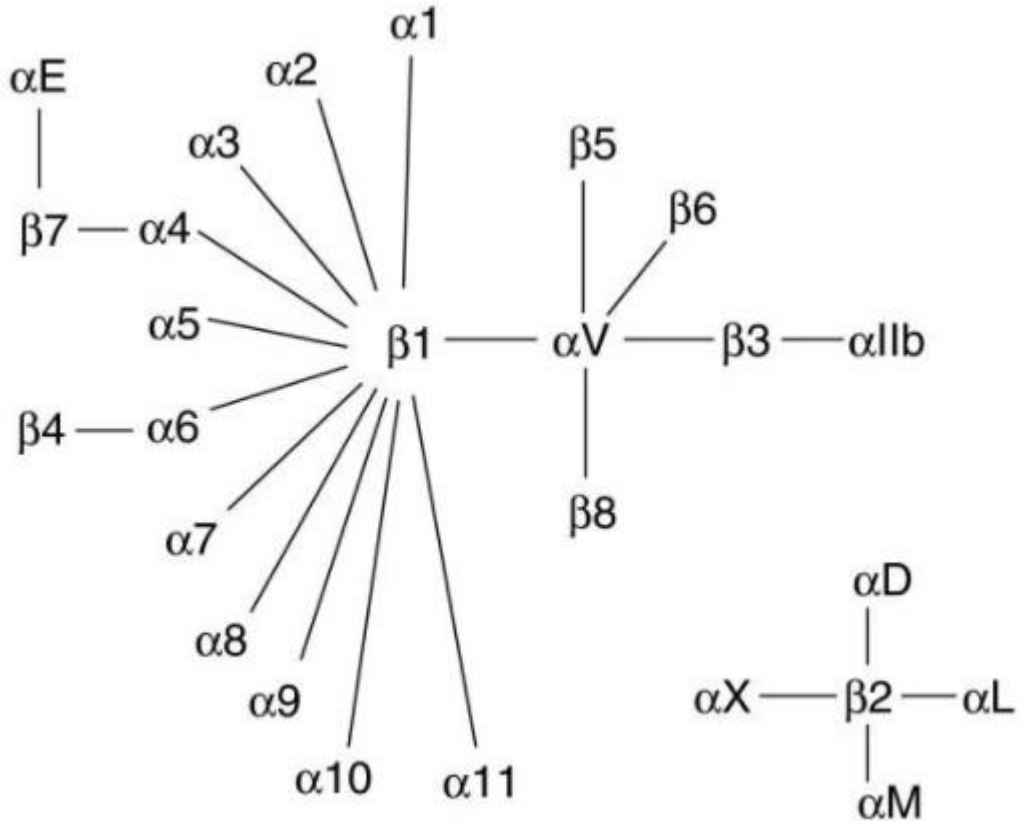


**Figure 1.4:** 18α and 8β chains combine to form 24 different αβ heterodimers (Takada et al., 2007).

Comparatively, the amino acid sequence of the $\alpha$ subunit differs from the β subunit although the two subunits associate non-covalently. The multi-domain extracellular portion of the α subunit encompasses two (2) calf domains, a thigh domain that conforms to the fold of IgG-like extracellular domain, and a β-propeller domain (Xiong et al., 2002). Furthermore, there is an αA domain that is not totally conserved in all integrins which when present is inserted into the loop of the β-propeller domain (Campbell and Humphries, 2011). On the other hand, the ectodomain of the β-subunit comprises of a $\beta$A or βI domain, a hybrid domain, a PSI-domain, four cysteine-rich EGF modules, and a β-tail domain (Xiong et al., 2002) (Figure

1.5). Integrins that can interact with collagens usually contain the αA domain. They include α1β1, α2β1, α10β1, and α11β1. The non-covalent association that exist between the α- and $\beta$-chains in integrins with αA domain is distinct in that the ligand binding head is formed between the αA and the βA domains. However, in the absence of αA, such ligand binding heads are formed between the β-propeller domain of the α-chain and the βA domain of the β-chain (Campbell and Humphries, 2011) (Figure 1.5).

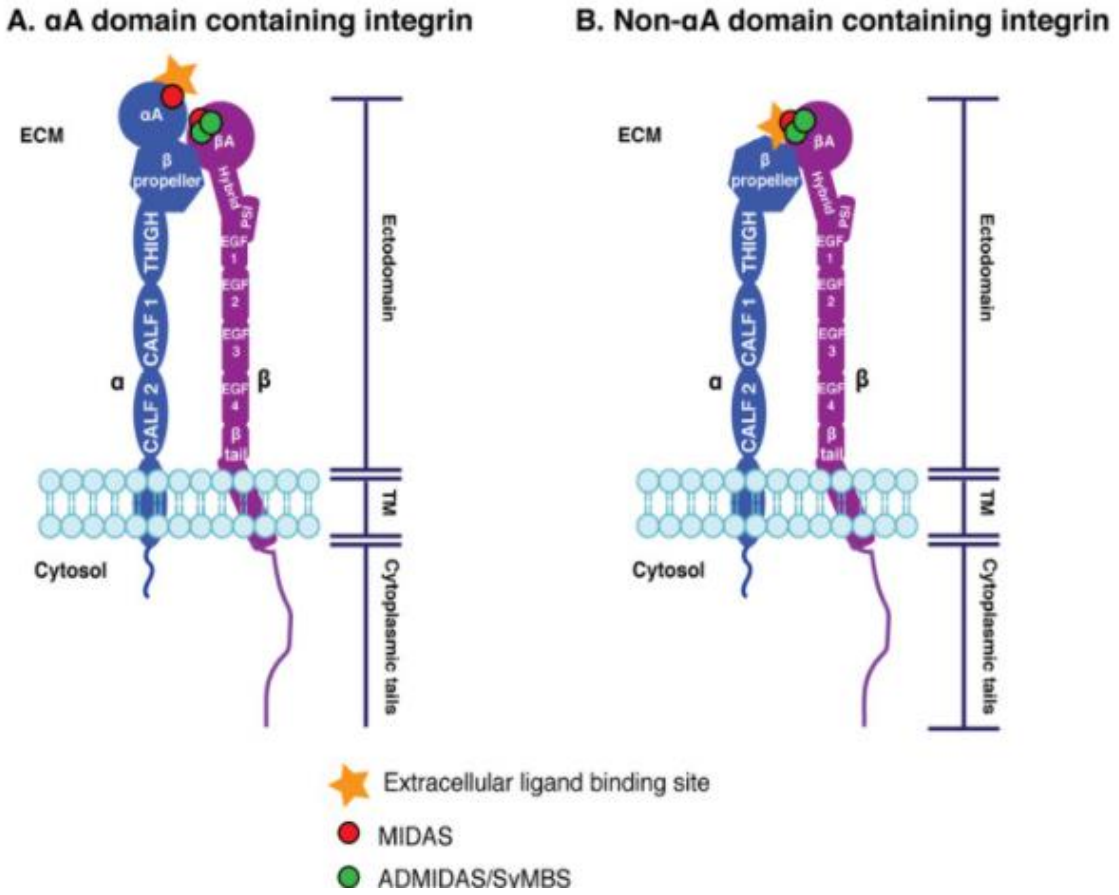


**Figure 1.5:** Non-covalent association between the α- and β- subunits of integrins that produce the ligand binding head (Kadry and Calderwood, 2020).

Importantly, the αA domain in the extracellular multi-domain region is critical to ligand binding. High resolution characterization revealed that the A-domain contain 'metal-ion dependent adhesion site (MIDAS)' capable of divalent-ion coordination (Lee et al., 1995). Further, there are three (3) other regions within the βA domain of the β subunit that can also coordinate interaction with charged residues on ligands in order to facilitate ligand binding to integrins. These include MIDAS, an adjacent MIDAS (ADMIDAS), and a synergistic metal-ion binding site (SyMBS) (Campbell and Humphries, 2011). For instance, the ligand binding head can coordinate interaction with the charged RGD-motif in ligands. An example of ligand that possesses this motif is the previously discussed P-II SVMPs. However, the ability of P-III SVMPs to interact with the ligand binding head of certain integrins may be due to the inherent ability of this head to coordinate interaction with the ECD motif that is present in P-III SVMPs.

### 1.3.1 Distribution of integrins

The distribution of integrins in organisms is a complex discourse. It is well known that all multicellular animals are capable of expressing integrins (Johnson et al., 2009). The reason could not be far-fetched. Multicellular cells clearly require some levels of cellular or tissue organization that can permit interactions and cellular communications. Such communications are pertinent to growth, survival, and cell motility. In plants, integrins are absent, but the role of integrin-like proteins have been shown. Katembe and colleagues immunocolocalized integrin-like molecules in the site of gravity perceptions in the root of *Arabidopsis* and the rhizoid of *Chara*. Their findings surmised that such integrin-like molecules may be integral part of plant plasma membrane (Katembe et al., 1997). Even though there are

integrin-like molecules in plants, there is no evidence that supports the existence of integrins in plants.

Arguably, integrins are found in multicellular animals but absent in multicellular plants; it is important to know that the connective tissue of plant and that of animal are quite disparate. While the ECM of animals are composed of hyaluronan, fibrous proteins, and GAGs; those of plants (cell wall) are composed of hemicellulose and pectin. This structural difference may account for the absence of integrins in plant.

From the evolutionary viewpoint, integrins were initially thought to be an animal-specific evolutionary innovation so that it is absent in other multicellular linages – such as plants, fungi, and choanoflagellates. However, in a recent report that analyzed the evolutionary history of Integrin Mediated Adhesion Complex (IMAC), it was shown that integrins have evolved earlier in eukaryotic evolution than previously thought. The presence of this complex has been reported in the most recent common ancestor of animals, fungi, and amoebae (Kang et al., 2020).

### 1.3.2 Biological functions of integrins

The ability of integrin to bind different ligands may account for its various biological role. The activation and inactivation of integrin are underlined by a complex interaction with ligands at the ligand binding head and the cytoplasmic tail of integrin. For instance, the cytoplasmic tail of the β-subunit contains certain unique sequence motifs which upon interaction with cytoplasmic adaptors are critical to cell migration, growth, survival, and wound healing process (Iwamoto and Calderwood, 2015; Morse et al., 2014). One of the most important binding partners of integrin is talin. This protein provide linkage access between integrins and actin cytoskeleton.

In epithelial cells, integrin plays vital role in epithelial cell – matrix interaction. It is such interaction that maintains the anchorage of epithelial cells to the basement membrane, thereby promoting growth and survival (Bouvard et al., 2003; Gilcrease, 2007). In addition, the continuous maintenance of such anchorage via cell-matrix interaction is also essential for the prevention of malignancy in epithelial cells. Integrins such as α3β1, α5β1, α6β1, α6β4, αvβ5, and αvβ6 are integrins expressed by the epithelial cells. The α3β1, α6β1, and α6β4 integrins can interact with laminin, a basement membrane component. In similar manner, α5β1 and αvβ6 can interact with fibronectin while αvβ5 can bind vitronectin (Gilcrease, 2007). All these interactions are essential component of integrin-mediated signaling that promote survival in epithelial cells.

On the other hand, there are certain integrin-mediated cell-matrix interactions that are essential for the maintenance of attachment during mitosis. It is important to note that the process of mitotic cell division cannot take place while maintaining anchorage. Thus, the type of anchorage needed for normal survival and prevention of malignant transformation is focal adhesion, while another called the reticular adhesion is required for the maintenance of attachment during mitotic cell division. Importantly, both type of adhesions are significantly coordinated by integrin-mediated signaling (Lock et al., 2018; Zuidema et al., 2018). Finally, integrin-mediated signaling can impact cell polarity which is critical to the formation of higher-order tissue architecture (Akhtar and Streuli, 2013).

### 1.3.3 The α2β1 Integrin

This α2β1 integrin is a heterodimer molecule whose monomeric compositions include the α2 integrin subunit and β1 subunit. The presence of highly conserved extracellular sequence has enabled the addition of this integrin to the 'I domain' integrins. The domain is so called due to its ability to predominantly bind collagen (Dickeson et al., 1998). Most of the features peculiar to the 'I' domain molecules are consistent with the 'I' domain of α2 subunit; including dependence on $Mg^{2+}$ and $Mn^{2+}$ (Elices et al., 1991; Inoue et al., 2003) and the presence of MIDAS motif which is essential for collagen binding (Kamata et al., 1999).

The α2β1 integrin is also called VLA-2, GPIa-IIa, and CD49b. the integrin was first known as a matrix receptor for collagens and laminins. However, it is now known that α2β1 integrin can interact with many matrix and nonmatrix ligand molecules (Madamanchi et al., 2014). Importantly, studies have identified that integrins possess higher binding affinity for collagen type I. This is due to the presence of high-affinity binding motif for α2β1 in collagen I. This motif is GFOGER motif found in type I, II, and XI collagens (Knight et al., 1998; Knight et al., 2000), and thus integrin α2β1 does not require activation that depends on an 'inside out signaling mechanism' before interacting with these collagens. Although the integrin α2β1 may require activation or a peculiar conformation, it can also interact with collagen III, IV, V, VI, XIII, XVI, and XXIII (Knight et al., 1998; Knight et al., 2000). In addition, the non-collagen ligands of α2β1 integrin includes laminin, perlecan, decorin, and some infectious agents (Chan and Hemler, 1993; Fleischmajer et al., 1991; Goyal et al., 2011; Sato et al., 2012).

α2β1 plays vital role in multicellular organisms. For instance, after injury, α2β1 integrin that is expressed on the surface of platelets can establish

the binding of platelet to collagen in the subendothelium (Kunicki et al., 1993). Such binding is required for wound healing. Experimental models have established that α2β1 integrin can bind to collagens I-VIII in a $Mg^{2+}$ - dependent fashion. In fact, patients who lack this integrin or possessing a reduced level as a result of low expression or autoimmunity have been described to exhibit impaired collagen-induced platelet aggregation and ultimately leading to abnormal bleeding (Nieuwenhuis et al., 1985).

On the other hand, the role of α2β1 integrin in angiogenesis and tubulogenesis has been established. Although the role is contradictory in both *in vivo and in vitro* experiments, there are indication that the α2β1 integrin is critical to angiogenic process (Senger et al., 1997). Apart from its role in blood vessel and tube formation, the role of α2β1 integrin was also established in late stage T-cell activation (Hemler, 1990). One of the most probable mechanisms through which this occur is via the ability of α2β1 integrin in a collagen-dependent process to inhibit the expression of Fas ligand and apoptosis in effector T cell (Gendron et al., 2003). In a particular study, memory Th cells that express α2β1 integrin become capacitated to influence the killing of intracellular bacteria via macrophage activation (Kapp et al., 2013). Put together, the α2β1 integrin expression in activated natural killer cell (Arase et al., 2001), mast cell (Edelson et al., 2006), $CD4^{+}$, $CD8^{+}$, and other immunological cells surmised that this integrin plays vital role in both innate and adaptive immunity. The role of α2β1 integrin in cancer progression seems contradicting. Some studies correlated the loss of α2β1 integrin to tumor proliferation and metastasis, while other studies stated otherwise. Nevertheless, it appears that α2β1 plays significant role in cancer. It is therefore of prime importance to establish the exact role of this integrin in cancer progression as the knowledge of its role can give room for drug development.

## 2.0 Objectives

In general, the overall goal of the current work is to contribute to the understanding of the roles of the disintegrin-like domain of bothropasin and more specifically, the ECD-integrin binding motif of this domain.

Thus the specific objectives include:

1. To express the BDC-GST-ECD (wild) and BDC-GST-ACD (mutant) proteins in E. coli;
2. To purify the wild and mutant proteins;
3. To study, through cell adhesion experiments, the capacity of these proteins to inhibit adhesion of α2β1 integrin (expressed in HUVECs) to collagen 1.

# 4. 3.0 Methodology

## 3.1 Cloning and site-directed mutagenesis

The full-length cDNA encoding the precursor of bothropasin disitegrin-like and cysteine-rich domains were cloned into pGEX-4T-1 vector (Assakura et al., 2003). This vector was received as a generous donation to our research group due to the fruitful collaboration with the group of Marina Assakura of "Laboratorio de Bioquimica e Biofisica, Instituto Butantan, Brasil".

In our group, Ike (2011) used QuikChange® II Site-Directed Mutagenesis Kit (Stratagene) to generate a mutant variant (pGEX-4T-1-BDC-ACD) from the wild type (pGEX-4T-1-BDC-ECD). The mutation involved glutamate (E) to alanine (A) transition in the integrin-binding motif. The clones were confirmed to be successful. Moreover, these plasmids were transformed into BL21(DE3) and DH5α strains of *E. coli* and some volume of the cultures were cryogenically stored in a -80 $^{0}$C freezer. Importantly, the stored cultures are highly resourceful for the current research.

## 3.2 Recombinant protein expression

Although the vectors were transformed into two strains of *E. coli*, Ike (2011) showed that the BL21(DE3) strain is more viable for protein expression. Thus, the current work utilized the BL21(DE3) strain for recombinant protein expression.

### 3.2.1 Plating

Agar medium was prepared according to the recommendation of our laboratory (LBFE). One liter stock usually contains tryptone (10g), yeast (5g), sodium chloride (10g), and agar (15g). Upon preparation, the medium was adjusted to pH 7.5 and sterilized in the autoclave. From the stock, 25 mL of the hot medium was transferred into falcon tube/tubes as the case may be for the number of plates to be prepared. As the medium became lukewarm, 50 µg/mL of ampicillin was added to the medium, mixed thoroughly and transferred to the petri dish. Upon cooling, the agar medium solidified.

From the cryogenically stored cultures, the plates were streaked accordingly. The whole procedure was carried out aseptically in fume hood to avoid contamination. The plates were then incubated overnight at 37 $^{0}$C.

### 3.2.2 Pre-inoculation

From the outcome of section 3.2.1, an isolated colony from the plate was used to pre-inoculate 10 mL Luria Bertani (LB) medium containing antibiotic ampicillin (50 µg/mL). This procedure was carried out aseptically in a fume chamber to avoid contamination. Furthermore, the pre-inoculated medium was placed in the sample holder of the incubator shaker. At 37 $^{0}$C and 200 rpm, the sample(s) was incubated for 16 hours.

### 3.2.3 Expression

The two cell cultures transformed with plasmids pGEX-4T-1-BDC-ACD and pGEX-4T-1-BDC-ECD have been in use until now in order to express the proteins in fusion with glutathione-S-transferase (GST). From the previous section (3.2.2), a specific volume of the pre-inoculum was used to inoculate a specific volume of freshly prepared LB medium that contains

antibiotic ampicillin (50 µg/mL). The ratio of the volume of the pre-inoculum to the volume of the freshly prepared LB is 1:100; so that for every 100 mL of LB medium, 1 mL of pre-inoculum was added. In addition, a ratio of 1: 5 was maintained between the volume of the medium and the volume of the conical flask used. The procedure was carried out in a fume cupboard to avoid contaminant.

From this foregoing, the freshly inoculated medium was then incubated at 37 $^0$C and 200 rpm until the cells reached the logarithm stage of growth. This growth was monitored by measuring the optical density (OD) of the culture at a wavelength of 600 nm in a DU® 800 spectrophotometer (Beckman Coulter). At OD between 0.6 and 0.8, gene expression was induced by the addition of 0.5 mM of Isopropyl-β-D-thiogalactopyranoside (IPTG). However, just before the induction, a 1 mL aliquot of the culture was collected in a 1.5 mL Eppendorf microtube for the purpose of expression analysis. This was designated $T_0$. Finally, having induced expression, the culture medium was incubated at 20 $^0$C and 200 rpm for about 16 hours.

### 3.2.4 Harvest of cell culture and sonication

16 hours after the induction of gene expression and protein synthesis under the conditions specified in section 3.2.3, 1 mL aliquot of the culture at $T_{16}$ was collected in a 1.5 mL Eppendorf microtube for analysis. The rest of the cultures were subjected to centrifugation at 4000 rpm and 4 $^0$C for 10 minutes in a Legend Mach 1.6 centrifuge (Sorvall) in order to harvest the cell. The supernatant (the culture medium) was discarded and the pellet was sonicated.

Ahead of sonication, a lysis buffer containing 50 nM Tris-HCl, 150 nM NaCl, and 1 % Triton at pH 7.4 was prepared. Moreover, the cell pellets

were first re-suspended in the lysis buffer and then placed in an ice bath for lysis. The lysis procedure involved an ultrasound technique and a vigorous agitation in a dismembrator model 500 (Fischer Scientific) for 10 minutes. The following conditions were ensured: 10 pulses of 59.9 seconds at 10 seconds interval and 23 % amplitude.

After sonication, the resulting cell lysate was centrifuged at 9000 rpm and 4 $^0$C for 30 minutes. The supernatant was expected to contain the soluble fraction of the protein and therefore collected for further treatment/study. In addition, an aliquot was collected from the supernatant and little portion of the pellet was also re-suspended in an ultra-pure water for analysis.

## 3.3 Purification and cleavage

Affinity chromatography was employed as a technique for purification. The column contained glutathione sepharose resin provided by Glutathione Sepharose 4 Fast Flow (GE Healthcare). The initial procedure involved the addition of 1 mL volume of resin into the column. The column was washed 4 times with deionized water and equilibrated with phosphate buffered saline (PBS) (140 nM Nacl, 2.7 nM KCl, 10 nM $Na_2HPO_4$, 1.8nM $KH_2PO_4$, pH 7.4). After equilibration of the resin, 10 mL of the supernatant was added to the resin and the set up was placed in an ice bath with gentle stirring for 1 hour in order to allow the GST-tagged proteins (GST-ACD and GST-ECD) to bind to the resin. After 1 hour of gentle stirring, the unbound protein was allowed to flow through the column and this was delineated as the void. On the other hand, the resin was collected into a 15 mL falcon tube, re-suspended in 1 mL PBS and centrifuged at 3000 xg and 4 $^0$C for 4 minutes. After this time and with the aid of a micro-pipette, the supernatant was gently removed and the process was repeated 10 times to wash the resin.

After the wash, the resin was transferred into the column and the resin-bound GST-tagged proteins were eluted with 1 mL of reduced glutathione (10 nM in PBS at pH 7.4) three times to obtain 3 eluents.

### 3.3.1 Dialysis

The procedure of dialysis was essential to remove the reduced glutathione previously used to elute the proteins. An Amicon filter stylishly embedded in a 50 mL falcon tube was used. The filter bed contains pores of 10,000 MW size of molecular dimension. The filter was washed 4 times with deionized water at 3000 xg and 4 $^0$C for 4 minutes and then equilibrated with 5 mL of PBS sample buffer. This was discarded after centrifugation.

Into the Amicon Filter, 2 mL of eluent was added and this was further diluted with 3 mL of PBS and centrifuged at 3000 xg and 4 $^0$C for 4 minutes. The procedure was repeated for 2 additional times and the sample in the filter was concentrated until 1 mL by continuous centrifugation. The dialyzed sample was finally transferred into a 1.5 mL Eppendorf microtube.

### 3.3.2 Cleavage of GST-tagged proteins

1 mL of purified and dialyzed GST-tagged protein was added to 500 µL resin, transferred into 1.5 mL Eppendorf tube, and 30 U of thrombin (Sigma) was added into the tube. The tube was then incubated at 37 $^0$C in a dry bath (HVD) for 2 hours and stirred at 150 rpm. After cleavage, the content of the tube was transferred into the column and the cleaved protein which was not bound to the resin was collected in the void. The collected protein was passed through a column containing 250 µL glutathione sepharose resin twice and the protein was collected. In addition, the resin-bound GST was eluted with reduced glutathione and dialyzed.

### 3.3.3 Removal of thrombin

From the cleaved protein, thrombin was removed by affinity column chromatography containing benzamidine resin from Benzamidine 4 Fast Flow (GE Healthcare). 250 µL of benzamidine resin was added into the column, washed 4 times with deionized water, and equilibrate with binding buffer (0.05 M Tris-HCl, 0.5 M NaCl, pH 7.4). The cleaved protein was then passed through the column in a single flow through event and the protein was collected. The thrombin in the sample was expected to interact with the benzamidine resin and this was eluted with an elution buffer (0.05 M glycine, pH 7.4).

## 3.4 Protein characterization

The process of expression, purification, dialysis, and cleavage were analyzed by SDS-PAGE and western blotting.

### 3.4.1 SDS-PAGE

15 % SDS polyacrylamide gel was prepared by the recommended protocol of our laboratory (LBFE). The fidelity of protein expression, purification, and dialysis were confirmed in the gel.

### 3.4.2 Western blotting

The western blot probe is a protein detection method whereby a specific antibody is targeted to protein of interest leading to detection of the protein (Renart et al., 1979).

The initial procedure involved resolution of protein sample by SDS-PAGE and blotting onto the surface of a nitrocellulose membrane. The blotting process involved the immersion of two pieces of sponge-like filter

paper into the transfer buffer (Tris 200 mM, glycine 50 mM, 15 % methanol). The nitrocellulose membrane and the gel were placed between the 2 papers like a sandwich and transferred in a transfer vat (Mini V8-GIBCO BRL – Life Technologies). The transfer was carried out at 150 V and 80 mA first for 1 hour and then 30 minutes.

Following the transfer, the membrane was stained with ponceau (0.5 % ponceau in 0.1 % acetic acid) for 5 minutes and washed with deionized water until the band became visible. Further, the membrane was incubated with a blocking solution for 1 hour. The blocking solution contained 5 % skimmed milk powder in TBS solution (50 mM Tris, 150 mM NaCl, pH 7.4). After 1 hour, the membrane was washed with TBST (50 mM Tris, 150 mM NaCl, 0.05% Tween 20, pH 7.4) 3 times at 5 minutes interval with a gentle stirring. The membrane was incubated with primary antibody (mouse anti-GST) for 1 hour, and the membrane was washed 3 times again with TBST. The secondary antibody (mouse anti-igG) was then added to the membrane and incubated for additional 1 hour. After this time, the membrane was washed with TBST 3 times and a revealing solution (1 SIGMA FASTTM BCIP / NBT tablet in 10 mL deionized water) was added to the membrane and covered from light by an aluminum foil until the bands were revealed.

## 3.5 Cell adhesion and inhibition assay

In this assay, the capacity of the wild and the mutant proteins to inhibit HUVECs adhesion to collagen was examined. HUVEC cells contain abundantly expressed α2β1 integrins. To confirm the viabilities of these cells and quantify the expression of these integrins, a flow cytometry technique was employed.

The cell adhesion experiment began with the coating of 96-well plates with collagen type I via incubation at 4 $^{0}$C overnight. However, the wells that depict the negative control were not incubated with collagen I, so that there is no adhesion between cells and this well (since the negative control lacked collagen I). On the second day, the wells were incubated at room temperature with blocking solution (0.1 % BSA and PBS 1X) for at least 1 hour and the wells were washed.

Further, HUVECs culture (1 x $10^{5}$ cells/mL) were pretreated with both wild and mutant proteins (1 to 10,000 nM ) at 37 $^{0}$C for 30 minutes. The solutions were then seeded appropriately in the 96-wells and incubated at 37 $^{0}$C for 45 minutes. After this time, each well was washed 4 times with PBS 1X until the negative controls have no cells. Moreover, the cells were fixed in the wells with formaldehyde 4 % for 10 minutes and washed 2 times with PBS 1X. In addition, the cells were stained with dye (2 µL of DAPI in 13 mL of PBS) for 10 minutes at room temperature and in a dark chamber. The cells were washed to remove excess dye and finally imaged.

# 4.0 Results and discussion

The aim of this chapter is to discuss the result of expression and purification of the wild and mutant proteins as well as the results of the cell adhesion and inhibition experiments.

## 4.1 Site-directed mutagenesis and cloning

Assakura group generously donated the pGEX-4T-1 containing cDNA that encode the precursor of the wild protein. Further, Ike (2011) employed site-directed mutagenesis to obtain a mutant variant (Figure 4.1). This successful approach led to the replacement of codon GAA that encode the glutamate residue by another codon GCT that encode alanine residue (Figure 4.3). Ike (2011) argued that the choice of alanine for glutamate replacement was due to the low reactivity of its side chain ($CH_3$).

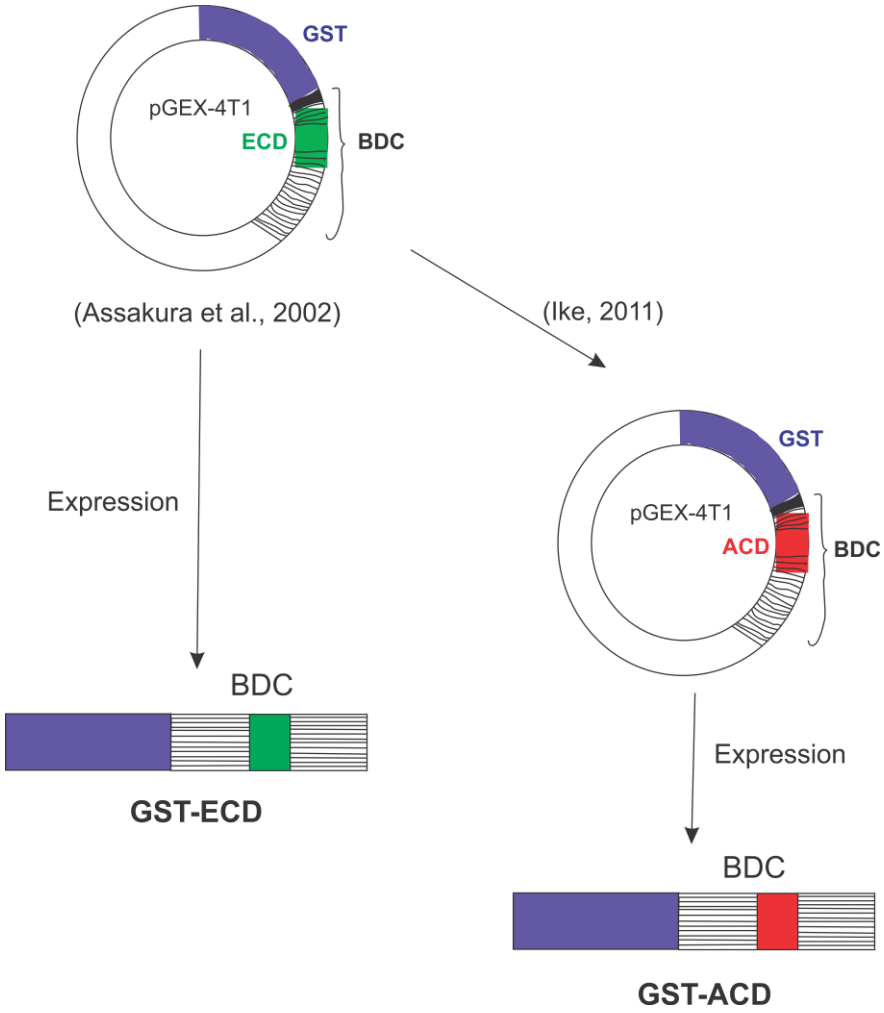


**Figure 4.1:** The figure depicts the overall approach employed by Ike (2011) to obtain the mutant variant from the wild protein donated by Assakura group. After generating a mutant precursor, this was cloned in pGEX-4T1. The size of this vector without the insert is 4900 bp. However, upon insertion of the precursors, the vectors containing the inserts for both the wild and mutant precursors have 5667 bp. The vectors were then transformed into BL21(DE3) and DH5α strains of *E. coli*.

In order to confirm that these strains still carry the desired vectors of the wild and mutant precursors, the following approach was employed. From the cryogenically stored cultures of the transformed *E. coli*, the cells were plated to obtain isolated colonies of the mutant and the wild type. Well isolated colony from each plate was then used to prepare a pre-inoculum to obtain the cells in a LB broth. Further, two (2) steps alkaline lysis procedure (Cellco Biotech Brazil) was employed to extract the plasmid DNA. The plasmid DNA extracted were then measured by nano drop (tech software). The results obtained showed that the BL21(DE3) strain for the wild and the mutant are 390.24 ng/µL and 459.87 ng/µL respectively; while in the DH5α, the plasmid DNA concentration obtained are 425.35 ng/µL and 244.28 ng/µL respectively. The result further corroborated the observation of Ike (2011) that the DH5α strain could propagate the vector better than the BL21(DE3) strain.

Due to the higher concentration of plasmid DNA extracted from the DH5α strain, these samples were then sent for Sanger sequencing. Upon receipt, the precursor nucleotide sequences obtained were aligned with 'Gapped BLAST and PSI-BLAST' to determine the presence of mutation (Altschul et al., 1997). Fortunately, the result (Figure 4.2) showed intact precursors that contain the GAA precursor codon for glutamate in the wild and GCT precursor codon for alanine in the mutant.

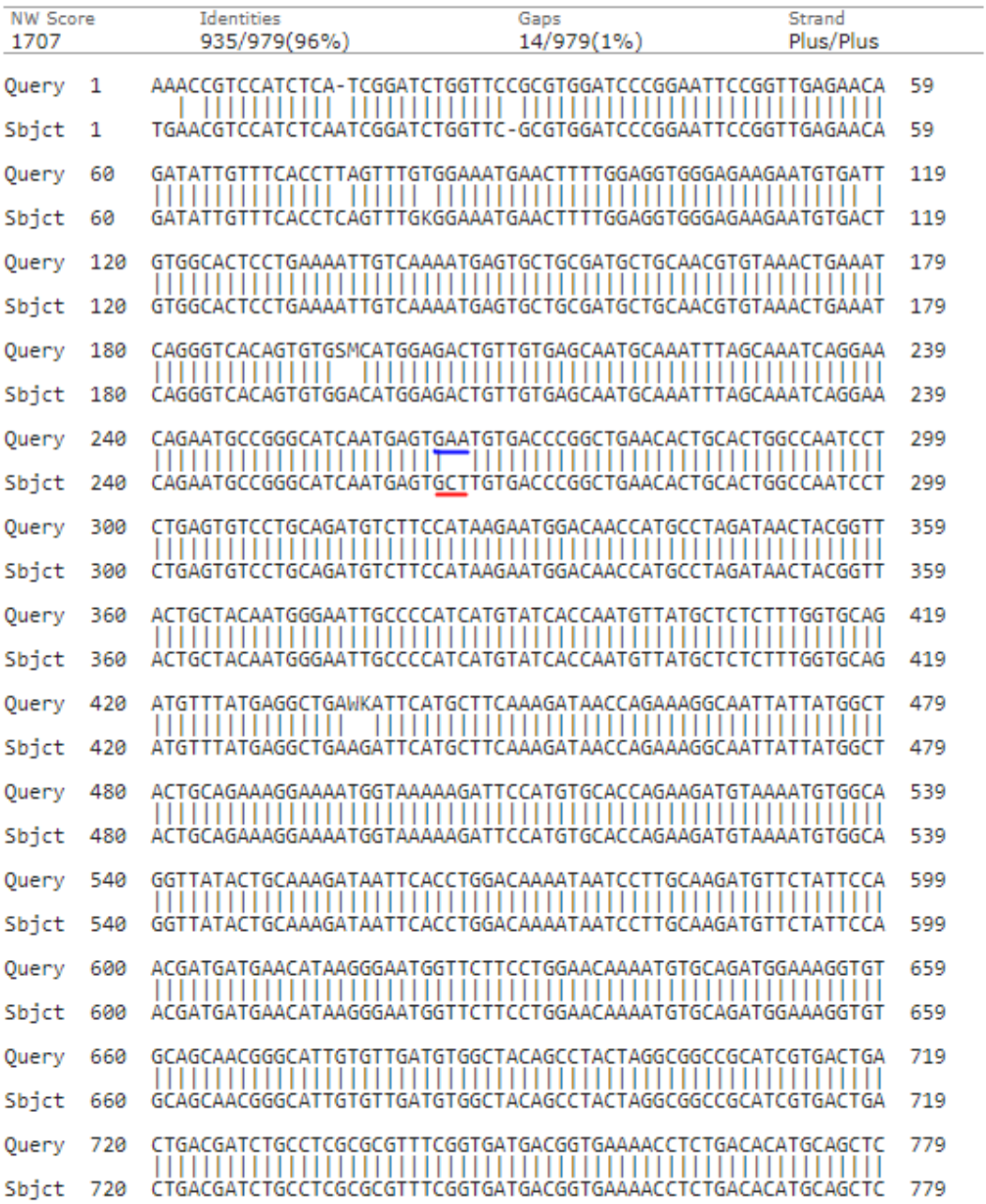


**Figure 4.2**: After employing Gapped BLAST and PSI-BLAST (Altschul et al., 1997) to align the precursor sequence of the wild and the mutant. Sequences between 240 and 299 showed the presence of GAA (underlined in blue) which is a precursor codon for glutamate in the wild (query), while the GCT (underlined red) is a precursor codon for alanine in the mutant (sbjct).

## 4.2 Protein expression

The transformed BL21(DE3) strain has a better yield for protein expression than the DH5α as observed by Ike (2011). Thus, in the current work, the BL21(DE3) strain was also used. This strain was cultured in two media to designate and differentiate the cells transformed with pGEX-4T-1-GST-BDC-ECD (wild) from the other transformed with pGEX-4T-1-GST-BDC-ACD (mutant). The proteins were expressed in fusion with Glutathione-S-Transferase (GST) according to the methods previously described in section 3. The molecular mass of the protein in fusion with GST is theoretically 52 kDa and this was also practically found in a region corresponding to this molecular mass as shown in Figure 4.4. This Figure also shows the protein expression for both the wild and the mutant. Lane 1 corresponds to the molecular mass marker; lane 2 and 6 are the samples taken before the induction of expression of the mutant and the wild respectively, this is called time zero (i.e T0) with regard to the time of expression. At this time, the recombinant protein (BDC) has not been synthesized, the cells were at their exponential phase of growth. After the induction of gene expression and protein synthesis, the cell continue to synthesize protein for a particular period of time – usually up to 16 hours. Samples collected at this specific time (T16) were also analyzed and lanes 3 and 7 correspond to T16¬ samples of the mutant and the wild respectively.

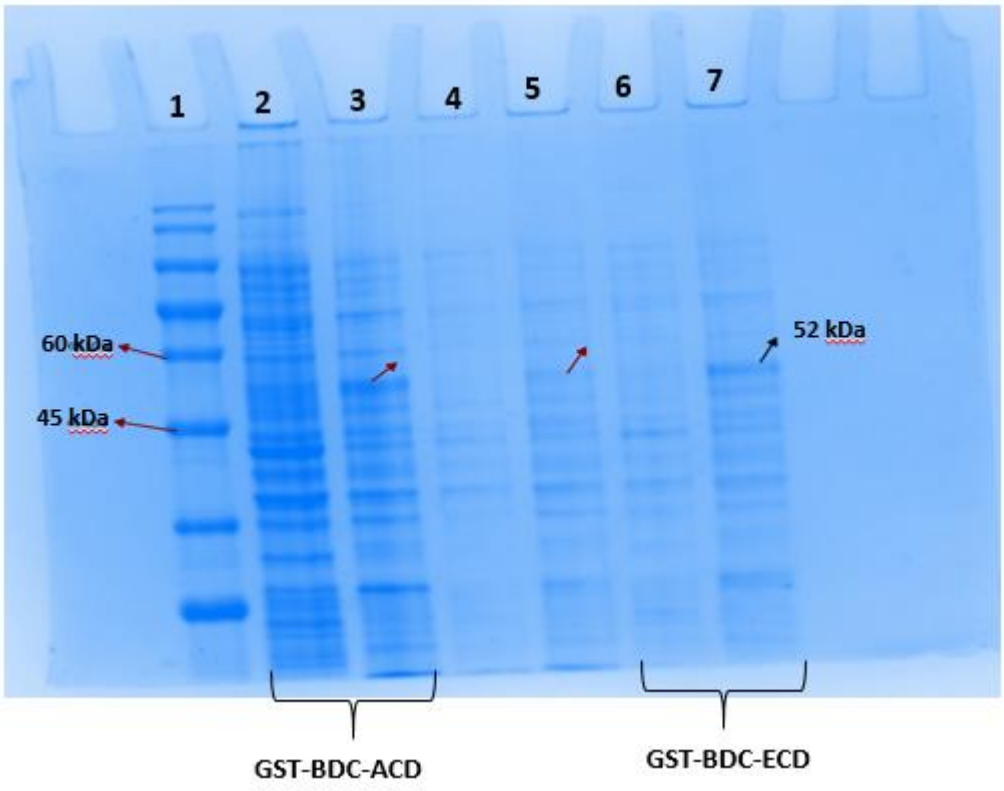


**Figure 4.3:** SDS-PAGE analysis of protein expression for both the wild and the mutant. Lane 1, molecular mass marker; lanes 2 and 6, samples taken before the induction of expression of the mutant and the wild respectively, this is called time zero (i.e $T_0$) with regard to the time of expression. Lanes 3 and 7, $T_{16}$ samples of the mutant and the wild respectively.

Furthermore, it is vital to determine the solubility of the proteins synthesized before the purification procedure. In order to this, the harvested cell culture were re-suspended in a lysis buffer and subjected to vigorous agitation by an ultrasound technique. This led to the lysis of the cell. The cell

lysates were then subjected to centrifugation to separate the soluble from the insoluble fractions. The insoluble fraction were trapped in the pellet while the desired soluble fraction were contained in the supernatant. The results for both the mutant and the wild were analyzed with SDS-PAGE (Figure 4.5). From the figure, all the lanes (i.e pellets and supernatants of the mutant and the wild proteins) contain the desired protein fraction. The protein in fusion with GST has a molecular mass of 52 kDa. Therefore bands found in the region of this molecular mass correspond to the protein. Importantly, the band that correspond to a region of 52 kDa was found in all the lanes 2, 3, 4, and 5. This therefore means that the expressed proteins were present in both soluble and insoluble fractions.

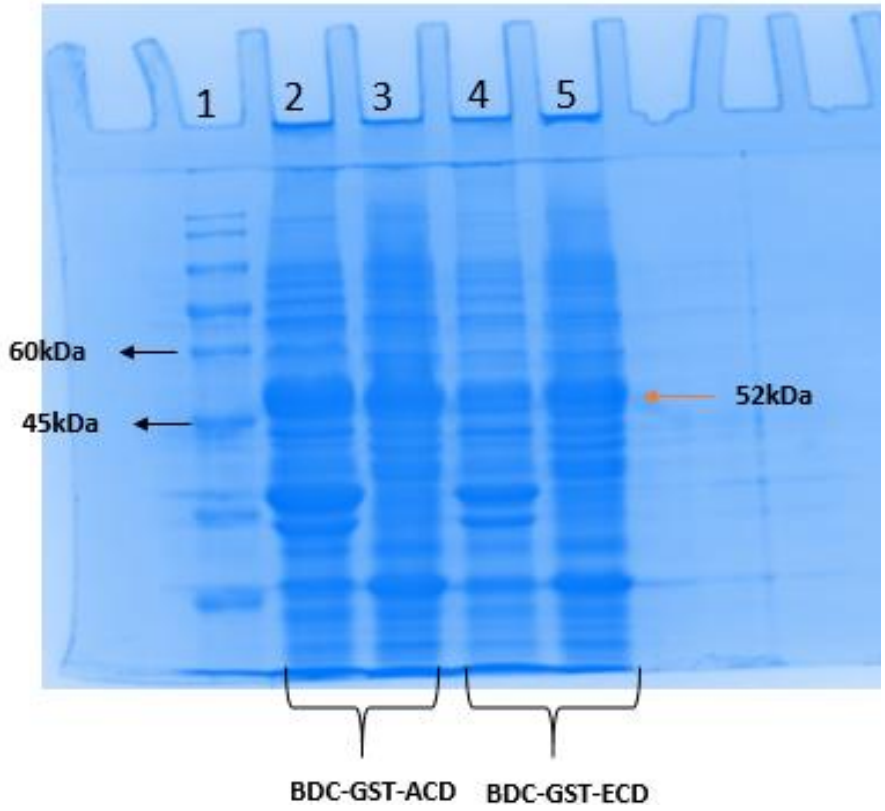


**Figure 4.4:** SDS-PAGE of the solubility test for the expressed proteins. Lane 1, molecular mass marker. Lanes 2 and 3; pellet and supernatant fractions of the mutant respectively. Lanes 4 and 5, pellet and the supernatant fractions of the wild respectively.

## 4.3 Protein purification

The soluble fractions of the proteins were purified by affinity chromatography techniques and the substance of the resin is glutathione sepharose. The proteins in fusion with GST interacted with the resin and others were washed off in the void. Finally the proteins were eluted with reduced glutathione and fractions from each step were collected for SDS-PAGE analysis.

The figure 4.6 represents the SDS-PAGE for the purification of the mutant (BDC-GST-ACD) and the wild (BDC-GST-ECD) proteins. The overall process was a double flow through process. In the first flow through (first binding), the supposed unbound proteins were collected in the void. The void was passed through the column in the second flow through process (second binding). After elution, there were four different eluents collected for the first binding and three different eluents were collected for the second binding in both the mutant and the wild categories. Lanes 6, 7, 8, 9 in the first bindings correspond to the 4 eluents; and lanes 6, 7, 8 in the second bindings correspond to the 3 eluents. In these lanes, prominent bands were present in regions corresponding to 52 kDa size and thus signified the presence of intact protein.

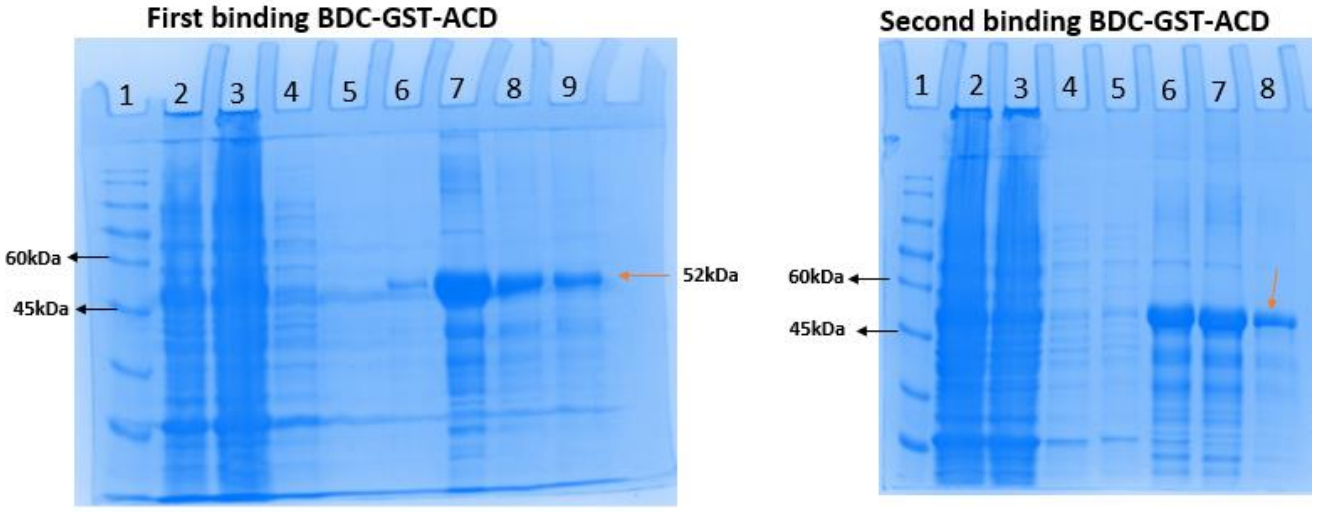

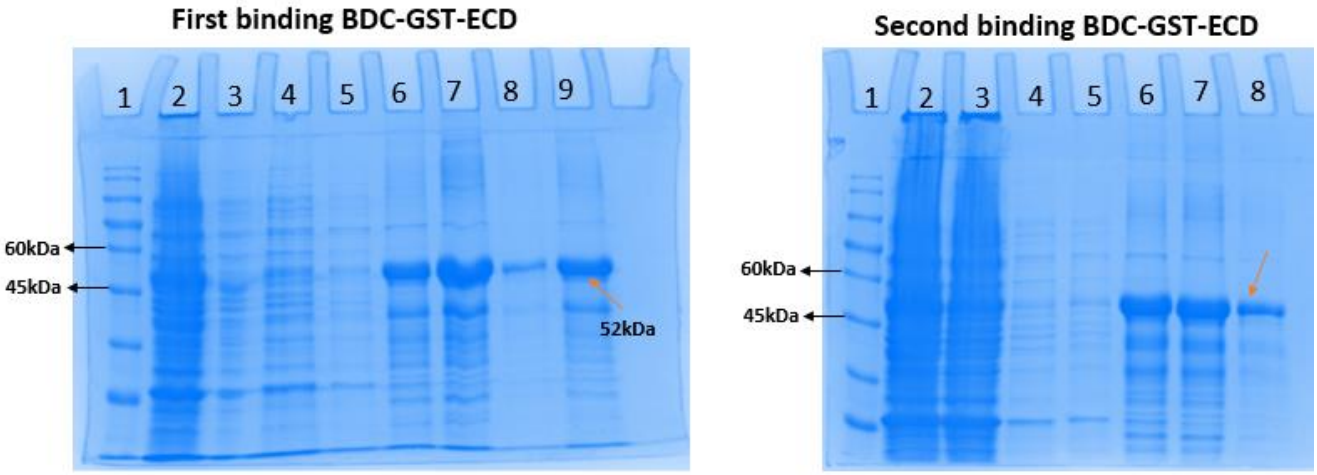


**Figure 4.5:** SDS-PAGE for the purification of the mutant (BDC-GST-ACD) and the wild (BDC-GST-ECD) proteins. Lanes 1, 2, 3, 4, and 5 corresponds to molecular mass marker, $T_0$, $T_{16,}$ void, and wash respectively. Lanes 6, 7, 8, and 9 in the first bindings correspond to the 4 eluents; and lanes 6, 7, 8 in the second bindings correspond to the 3 eluents.

The eluents contain significant volume of the elution buffer (reduced glutathione), it is therefore desirable that the samples are only contained in the sample buffer (PBS). In order to get rid of the eluant buffer, the eluents were dialyzed by Amicon Filter (10000 MW). After dialysis, the samples were again confirmed in SDS-PAGE (Figure 4.6).

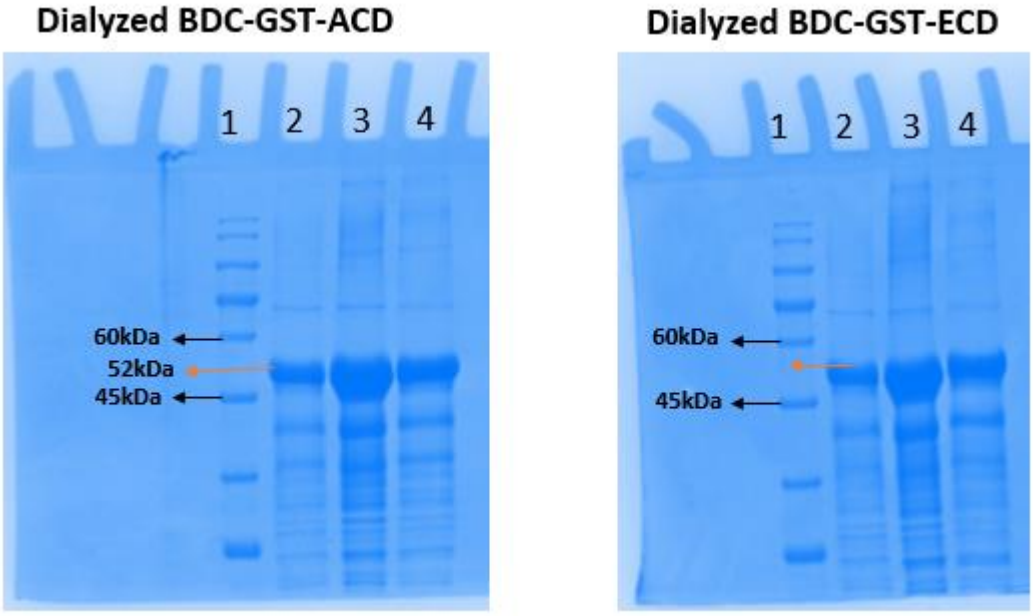


**Figure 4.6:** SDS-PAGE of the purified mutant and wild proteins dialyzed. Lane 1, molecular mass marker; lanes 2, 3, and 4, samples after dialysis.

### 4.3.1 Western blotting

It is known that the molecular mass of these proteins in fusion with GST is 52 kDa (Assakura et al., 2003). Further, Ike (2011) also confirmed that these proteins (wild and mutant) were present at bands that corresponded to this molecular mass. In the current work, the SDS-PAGE analysis also agrees with the report of Assakura and colleagues; and Ike (2011). To further show consistency, a western blotting assay was carried out. Anti-GST and anti-IgG antibodies both from mouse were used as primary and secondary antibodies respectively. The result of the probe is shown below (Figure 4.8). Regions of exactly 52 kDa correspond to the bands of the proteins. This further shows the consistency of the current work with the previous observations of Ike (2011) and Assakura et al. (2003). However, there are presence of other undesirable bands in all the lanes which signifies that some

of the protein fractions in fusion with GST are truncated and are therefore present as bands of different molecular mass.

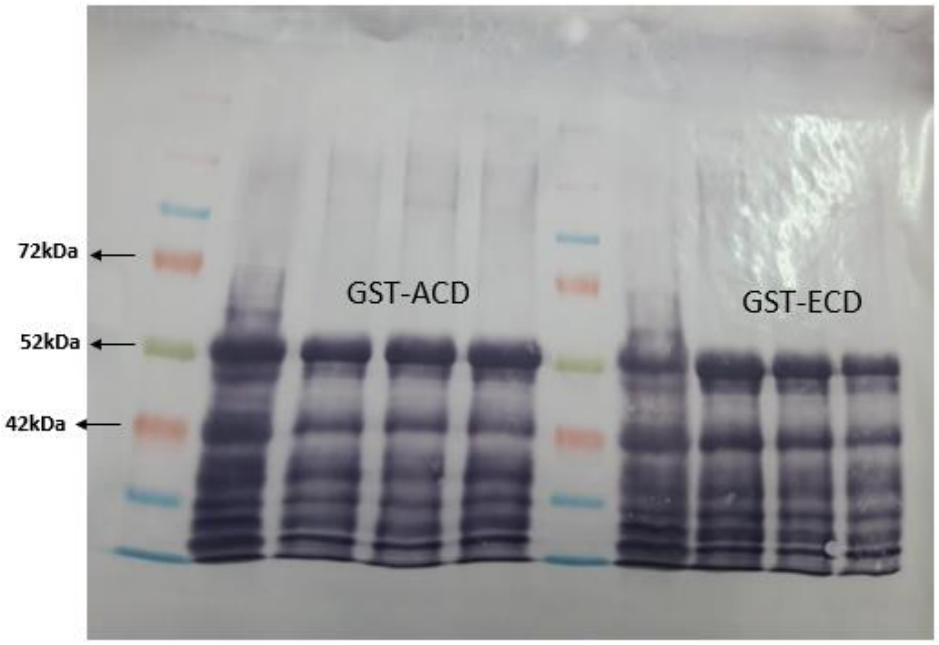


**Figure 4.7:** Western blotting of the samples with anti-GST primary antibody and anti-IgG secondary antibody.

## 4.4 Cleavage

The proteins in fusion with GST are soluble and contained in the sample buffer. Another aim of the current work is to obtain a GST-free protein and hence the need to cleave the fusion protein. Fortunately, the fusion proteins have cleavage site for thrombin. When thrombin was incubated with the proteins as described in the methodology, the cleavage was successful. Samples from the cleaved proteins and the eluted GST were analyzed (Figure 4.8).

In this figure, lane 1 corresponds to the molecular mass marker. Lanes 2, 3, and 4 are fractions of the mutant. Specifically, lane 2 corresponds to the fusion protein (GST-BDC-ACD) before cleavage. Upon cleavage, sample of the cleaved protein (BDC-ACD) was analyzed in lane 3. A region of about 30 kDa corresponds to the band of the protein. This is consistent with the report of Ike (2011) albeit this protein has a theoretic molecular mass of 26 kDa. In lane 4, the prominent band around 26 kDa correspond to the eluted GST. On the other hand, lanes 5, 6, 7, and 8 are lanes of the wild protein. Lane 5 corresponds to the fusion protein (GST-BDC-ECD) before the cleavage and a prominent band at 52 kDa could be observed in the gel. In lanes 6 and 7, the cleaved wild protein (BDC-ECD) was also observed at bands corresponding to a region of 30 kDa and consistent with the report of Ike (2011), while at about 26 kDa, a prominent band of the eluted GST could be observed. Unfortunately, in both the wild and the mutant, the cleaved proteins were contaminated with GST in a similar manner as the eluted GST were contaminated with the cleaved proteins.

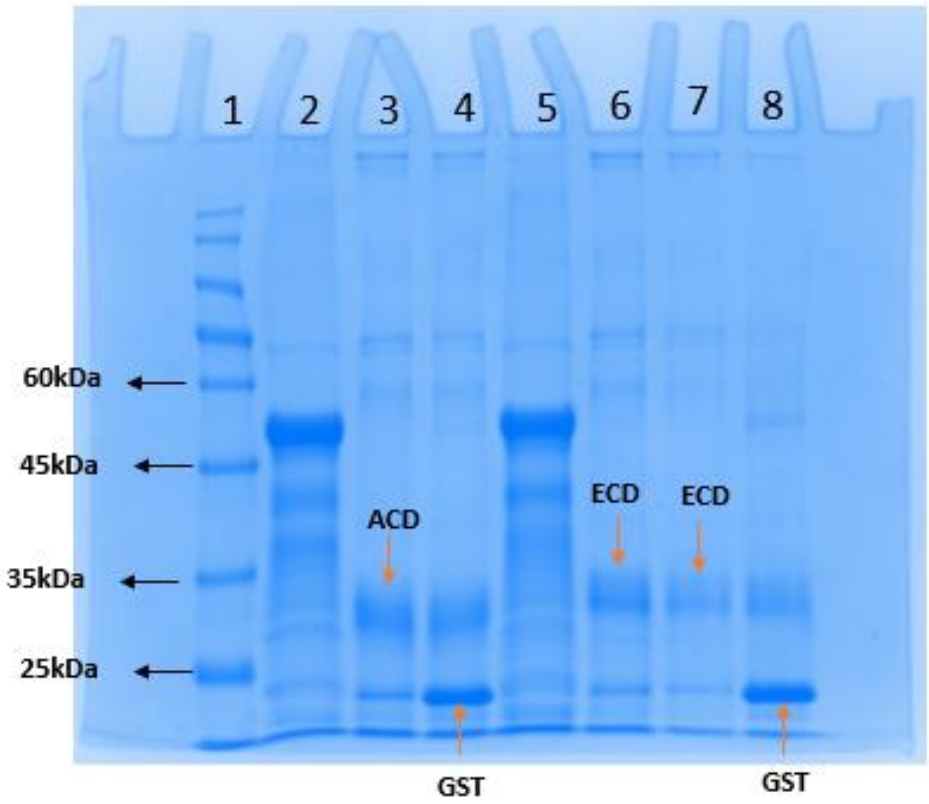


**Figure 4.8:** SDS-PAGE analysis of the cleavage experiment. Lane 1, molecular mass marker. Lanes 2, 3, and 4 are fractions of the mutant. Lane 2 corresponds to the fusion protein (GST-BDC-ACD) before cleavage. Upon cleavage, sample of the cleaved protein (BDC-ACD) was analyzed in lane 3. Lane 4, a prominent band around 26 kDa that correspond to the eluted GST. On the other hand, lanes 5, 6, 7, and 8 are lanes of the wild protein. Lane 5, the fusion protein (GST-BDC-ECD) before the cleavage. Lanes 6 and 7, the cleaved wild protein (BDC-ECD).

Since two bands of different molecular mass were present in the lanes of the cleaved proteins and the eluted GST, a western blotting probe was performed to confirm which of those two bands correspond to GST. Thus,

samples of the cleaved proteins and the eluted GST were subjected to western blot probe (Figure 4.9).

Using anti-GST primary and anti-IgG secondary antibodies, the exact band of the GST was identified in the contaminated lanes. In all the lanes, it now became lucid that the bands around 26 kDa is the GST since the band became prominent after western blotting. The bands around 30 kDa as shown in figure 4.8 are not revealed in figure 4.9 after western blotting. The unrevealed bands are the cleaved proteins while bands revealed after western blotting in this figure are GST.

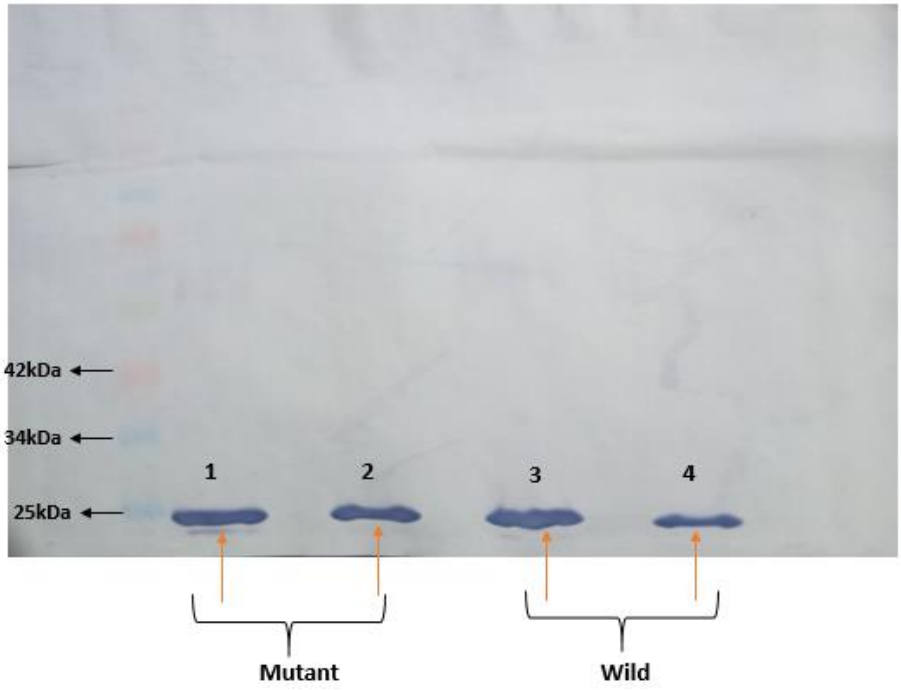


**Figure 4.9:** Western blot probe to confirm GST band.

### 4.4.1 Separation of GST from cleaved proteins by size exclusion chromatography

Ike (2011) noted that it would be difficult to separate the cleaved proteins and GST with both size exclusion chromatography and ion exchange chromatography due to the proximity of their molecular masses and their isoelectric points. In the current work, size exclusion chromatography was also employed to see the possibility of separating the GST from the cleaved proteins. The result obtained was consistent with the report of Ike (2011). When the peaks in the chromatograms were analyzed, the proteins were still contained in the same fraction (Figures 4.10 and 4.11), therefore the current work also conclude that, the size exclusion chromatography is not ideal for the separation of GST from the cleaved proteins.

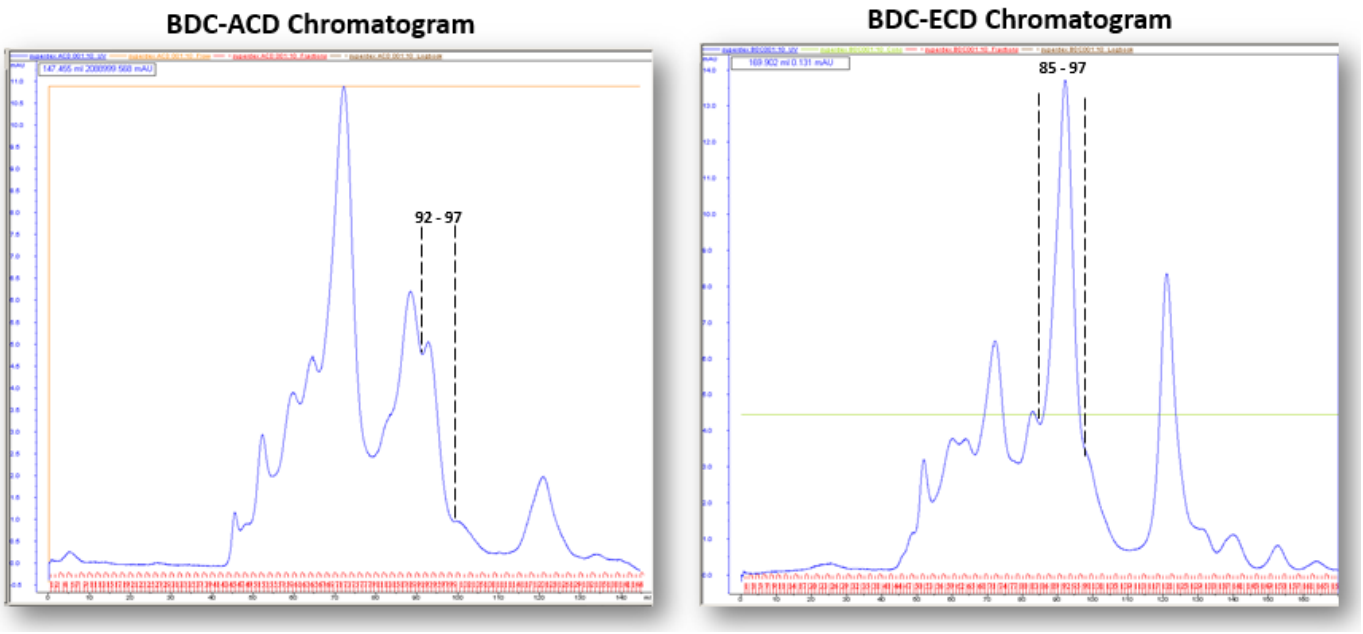


**Figure 4.10:** Chromatogram in a size exclusion column. In the chromatogram obtained for the mutant (BDC-ACD) above, the cleaved protein and the GST flowed out in fractions obtained from 92 to 97 minutes as shown in one of the peaks in figure 4.10. Similarly for the wild, the proteins and GST flowed out in fractions obtained from 85 to 97 minutes. Samples of all the peaks were analyzed in the SDS-PAGE to determine the exact peaks that contain the proteins and the GST (Figure 4.11). In both scenarios (i.e. mutant and the wild), the proteins are present with less contamination in lanes 4 for the mutant and lane 6 for the wild protein as shown in the gel. Apparently, the proteins were not separated from GST. Thus, the size exclusion chromatography is not ideal for the separation of GST from the proteins.

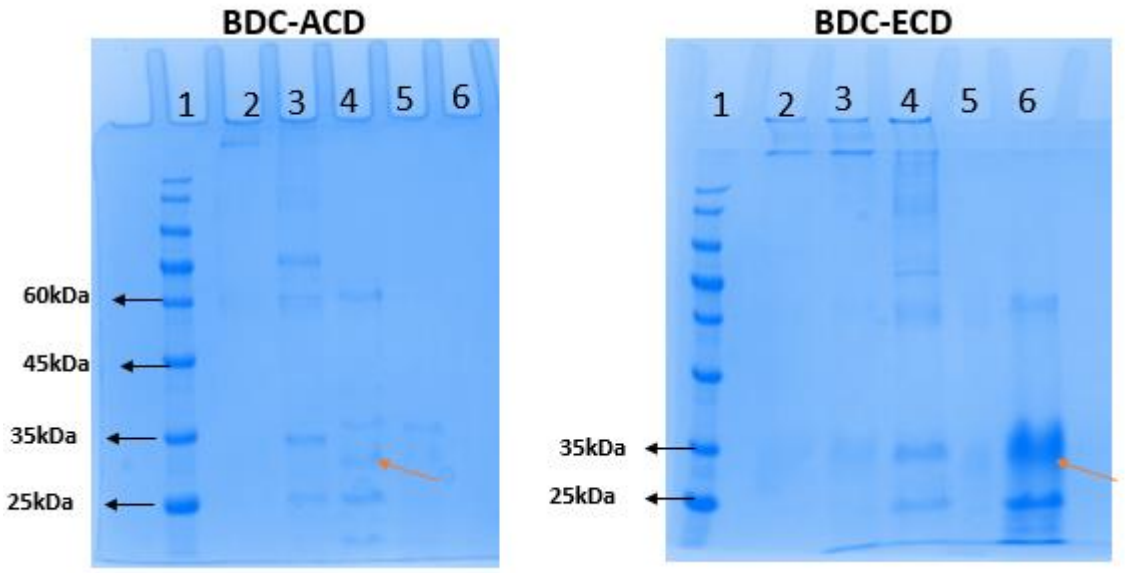


**Figure 4.11:** SDS-PAGE analysis of the peaks obtained in the chromatograms.

## 4.4.2 Removal of thrombin by affinity chromatography

Despite the inability to separate GST from the cleaved proteins, the current work also examined the contingency of removing thrombin from the cleaved fractions in order to obtain a thrombin-free sample. In the column, benzamidine formed the resin and was expected to interact with thrombin while the cleaved proteins would be collected in the void. However, samples collected were analyzed with SDS-PAGE and the result showed that the protein was not present in the void (Figure 4.12). The proteins must have undesirably interacted with the benzamidine column. The current observation is consistent with the report of Ike (2011) and the current work also conclude that the benzamidine-based affinity chromatography is not ideal for the removal of thrombin in the current work.

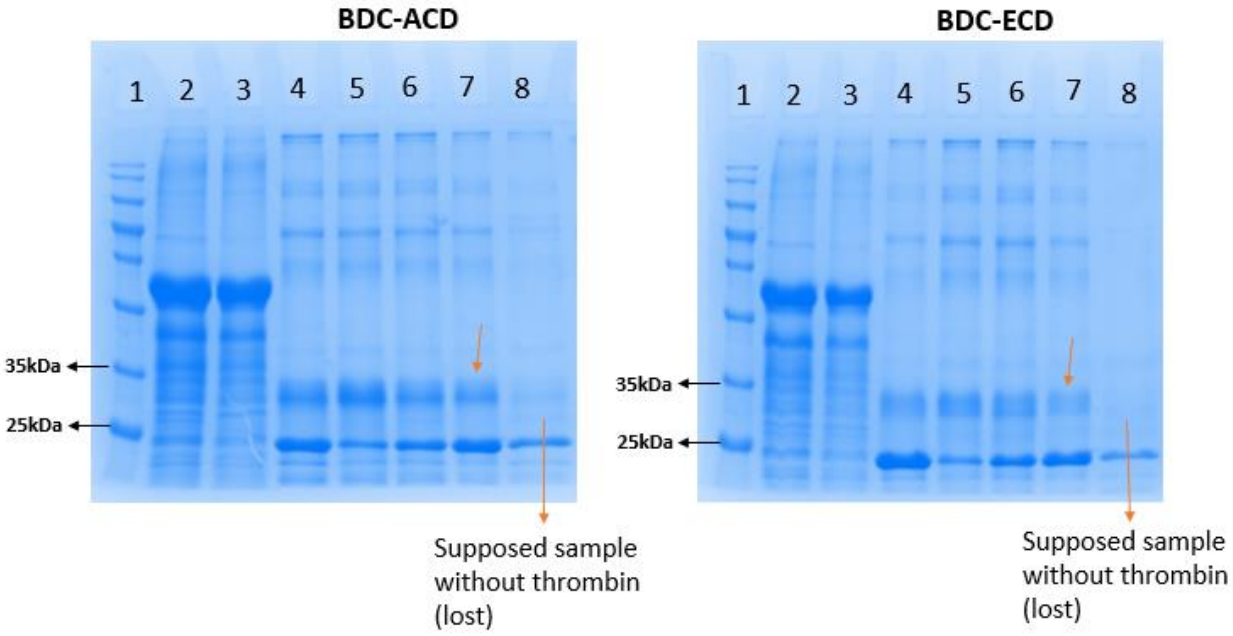


**Figure 4.12:** Gels showing the result of the thrombin removal experiment. In both mutant and the wild, lane 1 is the molecular mass. Lanes 2, and 3 are fusion proteins. Lanes 4, 5, 6, and 7 are cleaved proteins; a representative of the cleaved protein (lane 7; annotated with small arrow) was passed into the benzamidine column and the result obtained did not contain any band corresponding to a region where the protein could be found (lane 8). Although the result indicates that the proteins are lost, there are bands that correspond to GST.

### 4.4.3 Re-purification of GST

Due to the difficulties associated with the process of obtaining cleaved proteins, the current work therefore redefined its aim to use GST-tagged proteins instead of the cleaved ones. In addition, it also aimed at obtaining a pure GST in order to evaluate the effect of the GST tag in the cell adhesion experiment. In order to re-purify GST, previously eluted GST (although contaminated) was passed via glutathione sepharose resin, the void was allowed to run off while the GST was later re-eluted with reduced glutathione. The GST eluted was then dialyzed to remove the elution buffer; finally, samples were collected and analyzed with SDS-PAGE (Figure 4.13).

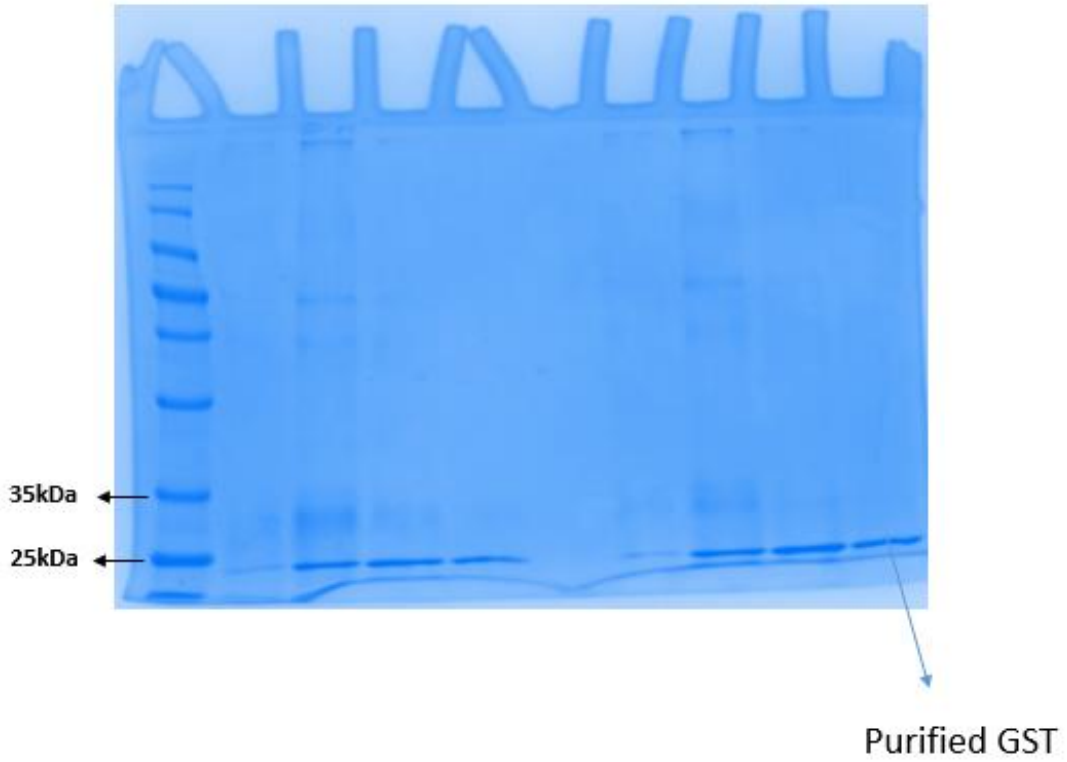


**Figure 4.13:** Re-purification of GST. In the gel, the last lane contains broad band corresponding to GST and shows less contamination.

## 4.5 Cell adhesion and inhibition assays

The cell adhesion and inhibition experiments represent the second part of the current work. The assays were carried out in collaboration with Professor Heloisa Sobreiro Selistre-de-Araujo (the PI of the Laboratory of Biochemistry and Molecular Biology at the Department of Physiological Sciences) and Dr. Kelli C. Micocci.

In the current work, the effect of glutamate mutation in the ECD-tripeptide integrin binding motif was examined. One of the important activities of botropasin disintegrin-like domain and other P-III members is their abilities to interact with integrins (Chang et al., 2017). The outcome of such interaction usually prevent the subsequent interaction of integrins with its other ligands. In biological systems, integrins play vital roles in cell to matrix interaction and maintenance of anchorage during somatic cell division (Gilcrease, 2007; Lock et al., 2018). Specifically, the integrins act as adhesive framework by interacting with the cytoskeleton of cells at one end and the extracellular matrix component (i.e., collagen) at another end.

Consequently, it is important to simulate the biological architecture of cell-matrix interaction *in vitro*. To achieve this, 96-wells plate was incubated with collagen 1 so that the surfaces were coated with collagen 1. Therefore upon incubation with cell lines containing integrins, they became adhered to the surface of these wells. In the current work, Human Umbilical Veins Endothelial Cells (HUVECs) were used as the cell model due to its ability to express α2β1 integrins abundantly. Once HUVECs medium is pre-treated with the wild protein (BDC-GST-ECD) and seeded into the plates, it is

expected that the protein would prevent HUVECs adhesion to the collagen 1 coated wells. However, it is not known how glutamate mutation and the presence of GST tag would impart this activity.

First, the viability of HUVECs and the presence of its expressed α2β1 integrins were confirmed via a flow cytometry technique. The result showed viable cells and abundantly expressed α2β1 integrins (Figure 4.14).

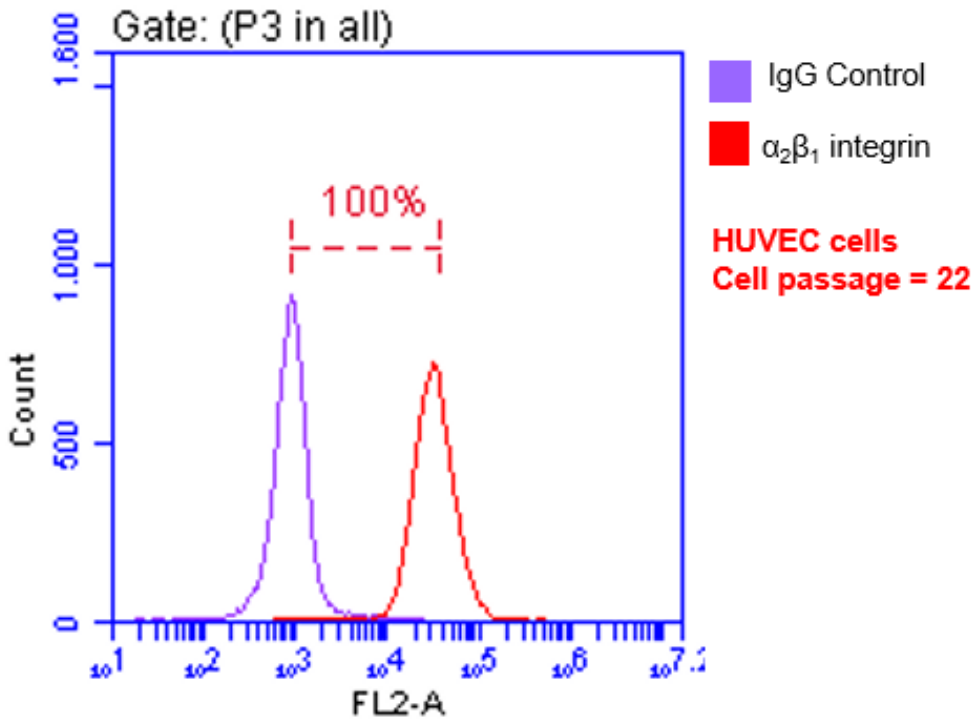


**Figure 4.14:** Flow cytometric analysis to show the presence of α2β1 integrins in HUVECs. Using IgG as control (100% as shown by the purple peak), the peak that corresponds to the integrin (red peak) shows abundance of these integrins in HUVECs.

Furthermore, the effect of glutamate mutation on the capacity of bothropasin disintegrin-like and cysteine-rich domains to inhibit cell adhesion was investigated. At 1000 nM, the wild protein containing the ECD motif and in fusion with GST inhibited 10.83 % of HUVECs from binding to collagen 1; while the mutant containing ACD motif inhibited 4.49 % of the cells. The effect of GST pretreatment on HUVECs show only 2.62 % of inhibition.

This experiment was repeated and also performed at a varying concentration (250 nM, 500 nM, 750 nM, 1000 nM, 2000 nM, and 5000 nM) in order to determine the consistency of the previous experiment and the best concentration for inhibition. The result obtained is shown in figure 4.15 below.

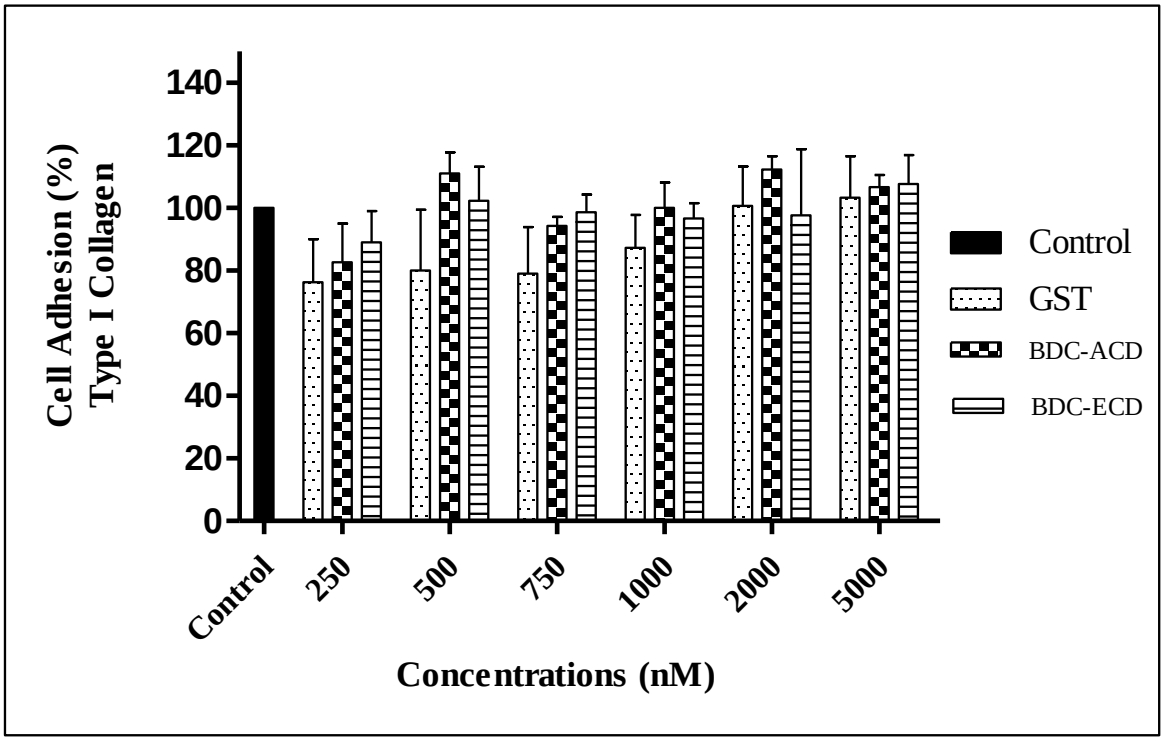


**Figure 4.15:** Graphical representation of HUVEC adhesion to collagen 1 after pretreatment with wild and mutant proteins at varying concentration.

At varying concentration, the capacity of protein to inhibit cell adhesion follow no defined pattern. The wild protein showed negligible inhibition of about 10 % at 250 nM, about 3 % at 1000 nM and 2000 nM in relative to the control. However, at 500 nM, 750 nM, and 5000 nM, the wild protein did not inhibit protein adhesion but rather appear to promote it. On the other hand, the mutant protein showed about 12 % inhibition at 250 nM, and about 4 % inhibition at 750 nM. However, at 500 nM, 1000 nM, 2000 nM, and 5000 nM, the mutant showed no inhibition. Further, when the cell was treated with GST only, its overall effect was not pronounced.

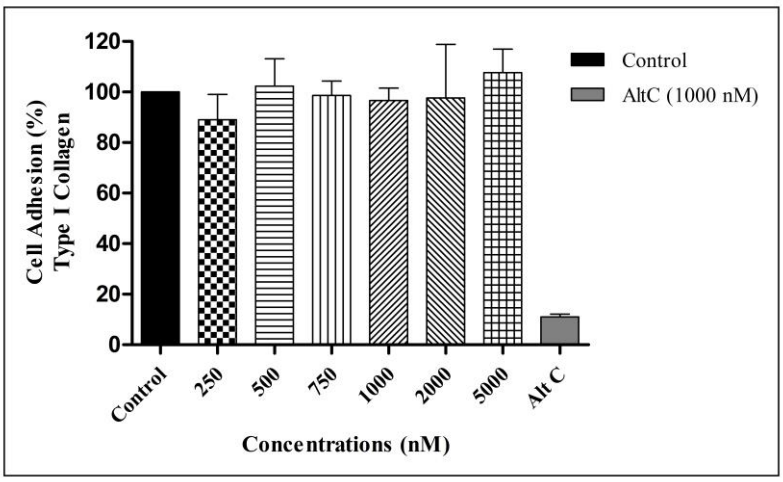


**BDC-GST-ECD (wild)**

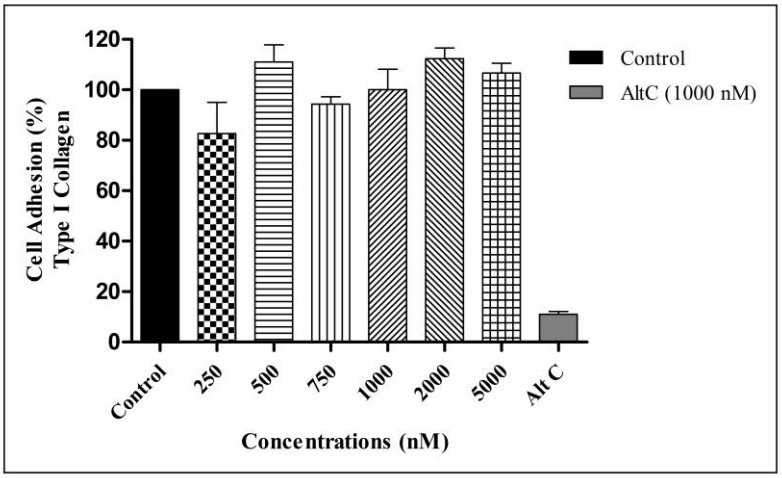


**BDC-GST-ACD (mutant)**

**Figure 4.16:** Graphical representation of HUVEC adhesion to collagen 1 after pretreatment with alternagin C at 100 nM; wild and mutant proteins at varying concentration.

Alternagin is a disintegrin-like protein purified from the venom of the Brazilian snake *Bothrops alternatus.* It contains the ECD-motif which was previously established to inhibit the interaction of α2β1 integrin with collagen 1 (do Santos *et al*., 2020). At 1000 nM, this protein was also treated with the cells and the result was compared with the wild and the mutant. In both scenarios, alternagin C showed more than 80 % inhibition capacity.

In general, the capacity of protein to inhibit adhesion followed no trend, therefore, the available date shows that the wild and the mutant proteins did not inhibit the adhesion of HUVECs to collagen I. One rationale behind this result could be that the ECD motif that guarantees the interaction of bothropasin with α2β1 integrin is different from the epitope that determines adhesion of α2β1 integrins in HUVEC to collagen 1. In fact, collagen 1 has been long shown to contain a high-affinity binding motif for α2β1 integrin. This motif is a GFOGER residues (Knight et al., 1998; Knight et al., 2000). If this is true in the case of α2β1 in HUVEC, then this may account for the reason why protein could not inhibit adhesion and give room for another possibility of co-localization. When ALT-C was labelled, Dos Santos and colleagues showed that ALT-C (an ECD-containing disintegrin-like protein from *Bothrops alternatus*) co-localized with α2β1 integrins in HUVECs adhered to COL1-coated slides (Dos Santos et al., 2020). This result further substantiates the possibility of co-localization although the authors also showed that ALT-C could inhibit HUVEC adhesion to collagen I.

Another possibility for no inhibition observed for both proteins may be due to the absence of the canonical RGD motif. In a more recent report, Danilucci and colleagues showed that DisBa-01 from *Bothrops alternatus* interacted with αvβ3 and markedly hampered HUVEC adhesion to extracellular matrix (Danilucci et al., 2019). It is therefore arguable that the ability of DisBa-01 to inhibit interaction of αvβ3 to extracellular matrix may be due to the presence of canonical RGD-integrin binding motif. Further, it has been long known in the literature that RGD-disintegrins are potent inhibitors of integrins (Niewiarowski et al., 1994). However, the nature of bothropasin-integrin interaction has not been shown.

Finally, the most convincing rationale may be attributed to the presence of GST tags. The proteins were purified and characterized in fusion with GST; although, the current data showed that GST alone did not significantly inhibit cell adhesion, its fusion with bothropasin might have affected the native/active conformation of this protein. Thus, the current data suggests further studies with proteins free from GST or other tags.

**Conclusion**

GST-BDC-ECD and GST-BDC-ACD did not inhibit cell adhesion. The current experiment was also carried out with GST, showing that GST does not significantly interfere with cell adhesion, which suggests that the non-inhibitory activity of proteins should not be attributed to GST. However, the presence of GST in the fusion proteins may be interfering with the folding of proteins leading to non-active proteins. Thus, with these experiments, it is not possible to infer functions in the ECD motif of the disintegrin. An interesting alternative would be to carry out cell adhesion experiments with free GST proteins, that is BDC-ECD and BDC-ACD.

## References

Akhtar, N., Streuli, C.H., 2013. An integrin-ILK-microtubule network orients cell polarity and lumen formation in glandular epithelium. Nat Cell Biol 15, 17-27.

Altschul, S.F., Madden, T.L., Schäffer, A.A., Zhang, J., Zhang, Z., Miller, W., Lipman, D.J., 1997. Gapped BLAST and PSI-BLAST: a new generation of protein database search programs. Nucleic Acids Res 25, 3389-3402.

Arase, H., Saito, T., Phillips, J.H., Lanier, L.L., 2001. Cutting edge: the mouse NK cell-associated antigen recognized by DX5 monoclonal antibody is CD49b (alpha 2 integrin, very late antigen-2). J Immunol 167, 1141-1144.

Assakura, M.T., Silva, C.A., Mentele, R., Camargo, A.C., Serrano, S.M., 2003. Molecular cloning and expression of structural domains of bothropasin, a P-III metalloproteinase from the venom of Bothrops jararaca. Toxicon 41, 217-227.

Baldo, C., Tanjoni, I., León, I.R., Batista, I.F., Della-Casa, M.S., Clissa, P.B., Weinlich, R., Lopes-Ferreira, M., Lebrun, I., Amarante-Mendes, G.P., Rodrigues, V.M., Perales, J., Valente, R.H., Moura-da-Silva, A.M., 2008. BnP1, a novel P-I metalloproteinase from Bothrops neuwiedi venom: biological effects benchmarking relatively to jararhagin, a P-III SVMP. Toxicon 51, 54-65.

Bjarnason, J.B., Fox, J.W., 1994. Hemorrhagic metalloproteinases from snake venoms. Pharmacol Ther 62, 325-372.

Bouvard, D., Vignoud, L., Dupé-Manet, S., Abed, N., Fournier, H.N., Vincent-Monegat, C., Retta, S.F., Fassler, R., Block, M.R., 2003. Disruption of focal adhesions by integrin cytoplasmic domain-associated protein-1 alpha. J Biol Chem 278, 6567-6574.

Calvete, J.J., Marcinkiewicz, C., Monleón, D., Esteve, V., Celda, B., Juárez, P., Sanz, L., 2005. Snake venom disintegrins: evolution of structure and function. Toxicon 45, 1063-1074.

Camacho, E., Villalobos, E., Sanz, L., Pérez, A., Escalante, T., Lomonte, B., Calvete, J.J., Gutiérrez, J.M., Rucavado, A., 2014. Understanding structural and functional aspects of PII snake venom metalloproteinases: characterization of BlatH1, a hemorrhagic dimeric enzyme from the venom of Bothriechis lateralis. Biochimie 101, 145-155.

Campbell, I.D., Humphries, M.J., 2011. Integrin structure, activation, and interactions. Cold Spring Harb Perspect Biol 3.

Carneiro, S.M., Zablith, M.B., Kerchove, C.M., Moura-da-Silva, A.M., Quissell, D.O., Markus, R.P., Yamanouye, N., 2006. Venom production in long-term primary culture of secretory cells of the Bothrops jararaca venom gland. Toxicon 47, 87-94.

Casewell, N.R., Wagstaff, S.C., Harrison, R.A., Renjifo, C., Wüster, W., 2011. Domain loss facilitates accelerated evolution and neofunctionalization of duplicate snake venom metalloproteinase toxin genes. Mol Biol Evol 28, 2637-2649.

Cesar, P.H.S., Braga, M.A., Trento, M.V.C., Menaldo, D.L., Marcussi, S., 2019. Snake Venom Disintegrins: An Overview of their Interaction with Integrins. Curr Drug Targets 20, 465-477.

Chalier, F., Mugnier, L., Tarbe, M., Aboudou, S., Villard, C., Kovacic, H., Gigmes, D., Mansuelle, P., de Pomyers, H., Luis, J., Mabrouk, K., 2020. Isolation of an Anti-Tumour Disintegrin: Dabmaurin-1, a Peptide Lebein-1-Like, from Daboia mauritanica Venom. Toxins (Basel) 12.

Chan, B.M., Hemler, M.E., 1993. Multiple functional forms of the integrin VLA-2 can be derived from a single alpha 2 cDNA clone:

interconversion of forms induced by an anti-beta 1 antibody. J Cell Biol 120, 537-543.

Chang, Y.T., Shiu, J.H., Huang, C.H., Chen, Y.C., Chen, C.Y., Chang, Y.S., Chuang, W.J., 2017. Effects of the RGD loop and C-terminus of rhodostomin on regulating integrin αIIbβ3 recognition. PLoS One 12, e0175321.

Clissa, P.B., Lopes-Ferreira, M., Della-Casa, M.S., Farsky, S.H., Moura-da-Silva, A.M., 2006. Importance of jararhagin disintegrin-like and cysteine-rich domains in the early events of local inflammatory response. Toxicon 47, 591-596.

Danilucci, T.M., Santos, P.K., Pachane, B.C., Pisani, G.F.D., Lino, R.L.B., Casali, B.C., Altei, W.F., Selistre-de-Araujo, H.S., 2019. Recombinant RGD-disintegrin DisBa-01 blocks integrin α(v)β(3) and impairs VEGF signaling in endothelial cells. Cell Commun Signal 17, 27.

de Souza, R.A., Díaz, N., Nagem, R.A., Ferreira, R.S., Suárez, D., 2016. Unraveling the distinctive features of hemorrhagic and non-hemorrhagic snake venom metalloproteinases using molecular simulations. J Comput Aided Mol Des 30, 69-83.

Dickeson, S.K., Walsh, J.J., Santoro, S.A., 1998. Binding of the alpha 2 integrin I domain to extracellular matrix ligands: structural and mechanistic differences between collagen and laminin binding. Cell Adhes Commun 5, 273-281.

Dos Santos, P.K., Altei, W.F., Danilucci, T.M., Lino, R.L.B., Pachane, B.C., Nunes, A.C.C., Selistre-de-Araujo, H.S., 2020. Alternagin-C (ALT-C), a disintegrin-like protein, attenuates alpha2beta1 integrin and VEGF receptor 2 signaling resulting in angiogenesis inhibition. Biochimie 174, 144-158.

Edelson, B.T., Stricker, T.P., Li, Z., Dickeson, S.K., Shepherd, V.L., Santoro, S.A., Zutter, M.M., 2006. Novel collectin/C1q receptor mediates mast cell activation and innate immunity. Blood 107, 143-150.

Elices, M.J., Urry, L.A., Hemler, M.E., 1991. Receptor functions for the integrin VLA-3: fibronectin, collagen, and laminin binding are differentially influenced by Arg-Gly-Asp peptide and by divalent cations. J Cell Biol 112, 169-181.

Fleischmajer, R., Fisher, L.W., MacDonald, E.D., Jacobs, L., Jr., Perlish, J.S., Termine, J.D., 1991. Decorin interacts with fibrillar collagen of embryonic and adult human skin. J Struct Biol 106, 82-90.

Fox, J.W., Serrano, S.M., 2005. Structural considerations of the snake venom metalloproteinases, key members of the M12 reprolysin family of metalloproteinases. Toxicon 45, 969-985.

Fox, J.W., Serrano, S.M., 2008. Insights into and speculations about snake venom metalloproteinase (SVMP) synthesis, folding and disulfide bond formation and their contribution to venom complexity. Febs j 275, 3016-3030.

Fox, J.W., Serrano, S.M., 2009. Timeline of key events in snake venom metalloproteinase research. J Proteomics 72, 200-209.

Gendron, S., Couture, J., Aoudjit, F., 2003. Integrin alpha2beta1 inhibits Fas-mediated apoptosis in T lymphocytes by protein phosphatase 2A-dependent activation of the MAPK/ERK pathway. J Biol Chem 278, 48633-48643.

Gilcrease, M.Z., 2007. Integrin signaling in epithelial cells. Cancer Lett 247, 1-25.

Goyal, A., Pal, N., Concannon, M., Paul, M., Doran, M., Poluzzi, C., Sekiguchi, K., Whitelock, J.M., Neill, T., Iozzo, R.V., 2011. Endorepellin, the angiostatic module of perlecan, interacts with both

the α2β1 integrin and vascular endothelial growth factor receptor 2 (VEGFR2): a dual receptor antagonism. J Biol Chem 286, 25947-25962.

Hemler, M.E., 1990. VLA proteins in the integrin family: structures, functions, and their role on leukocytes. Annu Rev Immunol 8, 365-400.

Herrera, C., Escalante, T., Voisin, M.B., Rucavado, A., Morazán, D., Macêdo, J.K., Calvete, J.J., Sanz, L., Nourshargh, S., Gutiérrez, J.M., Fox, J.W., 2015. Tissue localization and extracellular matrix degradation by PI, PII and PIII snake venom metalloproteinases: clues on the mechanisms of venom-induced hemorrhage. PLoS Negl Trop Dis 9, e0003731.

Hite, L.A., Jia, L.G., Bjarnason, J.B., Fox, J.W., 1994. cDNA sequences for four snake venom metalloproteinases: structure, classification, and their relationship to mammalian reproductive proteins. Arch Biochem Biophys 308, 182-191.

Humphries, J.D., Byron, A., Humphries, M.J., 2006. Integrin ligands at a glance. J Cell Sci 119, 3901-3903.

Hynes, R.O., 2002. Integrins: bidirectional, allosteric signaling machines. Cell 110, 673-687.

Inoue, O., Suzuki-Inoue, K., Dean, W.L., Frampton, J., Watson, S.P., 2003. Integrin alpha2beta1 mediates outside-in regulation of platelet spreading on collagen through activation of Src kinases and PLCgamma2. J Cell Biol 160, 769-780.

Iwamoto, D.V., Calderwood, D.A., 2015. Regulation of integrin-mediated adhesions. Curr Opin Cell Biol 36, 41-47.

Jangprasert, P., Rojnuckarin, P., 2014. Molecular cloning, expression and characterization of albolamin: a type P-IIa snake venom

metalloproteinase from green pit viper (Cryptelytrops albolabris). Toxicon 79, 19-27.

Johnson, M.S., Lu, N., Denessiouk, K., Heino, J., Gullberg, D., 2009. Integrins during evolution: evolutionary trees and model organisms. Biochim Biophys Acta 1788, 779-789.

Kadry, Y.A., Calderwood, D.A., 2020. Chapter 22: Structural and signaling functions of integrins. Biochim Biophys Acta Biomembr 1862, 183206.

Kamata, T., Liddington, R.C., Takada, Y., 1999. Interaction between collagen and the alpha(2) I-domain of integrin alpha(2)beta(1). Critical role of conserved residues in the metal ion-dependent adhesion site (MIDAS) region. J Biol Chem 274, 32108-32111.

Kang, S., Tice, A.K., Stairs, C.W., Lahr, D.J.G., Jones, R.E., Brown, M.W., 2020. The integrin-mediated adhesome complex, essential to multicellularity, is present in the most recent common ancestor of animals, fungi, and amoebae. 2020.2004.2029.069435.

Kapp, T.G., Rechenmacher, F., Sobahi, T.R., Kessler, H., 2013. Integrin modulators: a patent review. Expert Opin Ther Pat 23, 1273-1295.

Katembe, W.J., Swatzell, L.J., Makaroff, C.A., Kiss, J.Z., 1997. Immunolocalization of integrin-like proteins in Arabidopsis and Chara. Physiol Plant 99, 7-14.

Knight, C.G., Morton, L.F., Onley, D.J., Peachey, A.R., Messent, A.J., Smethurst, P.A., Tuckwell, D.S., Farndale, R.W., Barnes, M.J., 1998. Identification in collagen type I of an integrin alpha2 beta1-binding site containing an essential GER sequence. J Biol Chem 273, 33287-33294.

Knight, C.G., Morton, L.F., Peachey, A.R., Tuckwell, D.S., Farndale, R.W., Barnes, M.J., 2000. The collagen-binding A-domains of integrins alpha(1)beta(1) and alpha(2)beta(1) recognize the same specific

amino acid sequence, GFOGER, in native (triple-helical) collagens. J Biol Chem 275, 35-40.

Kunicki, T.J., Orchekowski, R., Annis, D., Honda, Y., 1993. Variability of integrin alpha 2 beta 1 activity on human platelets. Blood 82, 2693-2703.

Labat-Robert, J., 1992. [Integrins]. Pathol Biol (Paris) 40, 883-888.

Lee, J.O., Rieu, P., Arnaout, M.A., Liddington, R., 1995. Crystal structure of the A domain from the alpha subunit of integrin CR3 (CD11b/CD18). Cell 80, 631-638.

Lino, R.L.B., Dos Santos, P.K., Pisani, G.F.D., Altei, W.F., Cominetti, M.R., Selistre-de-Araújo, H.S., 2019. Alphavbeta3 integrin blocking inhibits apoptosis and induces autophagy in murine breast tumor cells. Biochim Biophys Acta Mol Cell Res 1866, 118536.

Lock, J.G., Jones, M.C., Askari, J.A., Gong, X., Oddone, A., Olofsson, H., Göransson, S., Lakadamyali, M., Humphries, M.J., Strömblad, S., 2018. Reticular adhesions are a distinct class of cell-matrix adhesions that mediate attachment during mitosis. Nat Cell Biol 20, 1290-1302.

Madamanchi, A., Santoro, S.A., Zutter, M.M., 2014. α2β1 Integrin. Adv Exp Med Biol 819, 41-60.

Mandelbaum, F.R., Reichel, A.P., Assakura, M.T., 1982. Isolation and characterization of a proteolytic enzyme from the venom of the snake Bothrops jararaca (Jararaca). Toxicon 20, 955-972.

Markland, F.S., Jr., Swenson, S., 2013. Snake venom metalloproteinases. Toxicon 62, 3-18.

Masuda, S., Ohta, T., Kaji, K., Fox, J.W., Hayashi, H., Araki, S., 2000. cDNA cloning and characterization of vascular apoptosis-inducing protein 1. Biochem Biophys Res Commun 278, 197-204.

Molina Molina, D.A., Guerra-Duarte, C., Naves de Souza, D.L., Costal-Oliveira, F., Ávila, G.R., Soccol, V.T., Machado-de-Ávila, R.A.,

Chávez-Olórtegui, C., 2018. Identification of a linear B-cell epitope in the catalytic domain of bothropasin, a metalloproteinase from Bothrops jararaca snake venom. Mol Immunol 104, 20-26.

Morse, E.M., Brahme, N.N., Calderwood, D.A., 2014. Integrin cytoplasmic tail interactions. Biochemistry 53, 810-820.

Moura-da-Silva, A.M., Almeida, M.T., Portes-Junior, J.A., Nicolau, C.A., Gomes-Neto, F., Valente, R.H., 2016. Processing of Snake Venom Metalloproteinases: Generation of Toxin Diversity and Enzyme Inactivation. Toxins (Basel) 8.

Muniz, J.R., Ambrosio, A.L., Selistre-de-Araujo, H.S., Cominetti, M.R., Moura-da-Silva, A.M., Oliva, G., Garratt, R.C., Souza, D.H., 2008. The three-dimensional structure of bothropasin, the main hemorrhagic factor from Bothrops jararaca venom: insights for a new classification of snake venom metalloprotease subgroups. Toxicon 52, 807-816.

Nieuwenhuis, H.K., Akkerman, J.W., Houdijk, W.P., Sixma, J.J., 1985. Human blood platelets showing no response to collagen fail to express surface glycoprotein Ia. Nature 318, 470-472.

Niewiarowski, S., McLane, M.A., Kloczewiak, M., Stewart, G.J., 1994. Disintegrins and other naturally occurring antagonists of platelet fibrinogen receptors. Semin Hematol 31, 289-300.

Olaoba, O.T., Karina Dos Santos, P., Selistre-de-Araujo, H.S., Ferreira de Souza, D.H., 2020. Snake Venom Metalloproteinases (SVMPs): A structure-function update. Toxicon X 7, 100052.

Oliveira, A.K., Paes Leme, A.F., Asega, A.F., Camargo, A.C., Fox, J.W., Serrano, S.M., 2010. New insights into the structural elements involved in the skin haemorrhage induced by snake venom metalloproteinases. Thromb Haemost 104, 485-497.

Queiroz, L.S., Santo Neto, H., Assakura, M.T., Reichl, A.P., Mandelbaum, F.R., 1985. Pathological changes in muscle caused by haemorrhagic

and proteolytic factors from Bothrops jararaca snake venom. Toxicon 23, 341-345.

Ramos, O.H., Kauskot, A., Cominetti, M.R., Bechyne, I., Salla Pontes, C.L., Chareyre, F., Manent, J., Vassy, R., Giovannini, M., Legrand, C., Selistre-de-Araujo, H.S., Crépin, M., Bonnefoy, A., 2008. A novel alpha(v)beta (3)-blocking disintegrin containing the RGD motive, DisBa-01, inhibits bFGF-induced angiogenesis and melanoma metastasis. Clin Exp Metastasis 25, 53-64.

Renart, J., Reiser, J., Stark, G.R., 1979. Transfer of proteins from gels to diazobenzyloxymethyl-paper and detection with antisera: a method for studying antibody specificity and antigen structure. Proc Natl Acad Sci U S A 76, 3116-3120.

Sato, Y., Morimoto, K., Kubo, T., Yanagihara, K., Seyama, T., 2012. High mannose-binding antiviral lectin PFL from Pseudomonas fluorescens Pf0-1 promotes cell death of gastric cancer cell MKN28 via interaction with α2-integrin. PLoS One 7, e45922.

Senger, D.R., Claffey, K.P., Benes, J.E., Perruzzi, C.A., Sergiou, A.P., Detmar, M., 1997. Angiogenesis promoted by vascular endothelial growth factor: regulation through alpha1beta1 and alpha2beta1 integrins. Proc Natl Acad Sci U S A 94, 13612-13617.

Takada, Y., Ye, X., Simon, S., 2007. The integrins. Genome Biol 8, 215.

Takeda, S., Takeya, H., Iwanaga, S., 2012. Snake venom metalloproteinases: structure, function and relevance to the mammalian ADAM/ADAMTS family proteins. Biochim Biophys Acta 1824, 164-176.

Wang, S.H., Shen, X.C., Yang, G.Z., Wu, X.F., 2003. cDNA cloning and characterization of Agkistin, a new metalloproteinase from Agkistrodon halys. Biochem Biophys Res Commun 301, 298-303.

Xiong, J.P., Stehle, T., Zhang, R., Joachimiak, A., Frech, M., Goodman, S.L., Arnaout, M.A., 2002. Crystal structure of the extracellular segment of integrin alpha Vbeta3 in complex with an Arg-Gly-Asp ligand. Science 296, 151-155.

Zuidema, A., Wang, W., Kreft, M., Te Molder, L., Hoekman, L., Bleijerveld, O.B., Nahidiazar, L., Janssen, H., Sonnenberg, A., 2018. Mechanisms of integrin αVβ5 clustering in flat clathrin lattices. J Cell Sci 131.